Iron Catalyzed C-C Coupling Reactions

Mechanistic Investigations

Anna Hedström

UNIVERSITY OF GOTHENBURG

Department of Chemistry and Molecular Biology
University of Gothenburg
2013

Doctoral Thesis

Submitted for partial fulfillment of the requirements for the degree of
Doctor of Philosophy in Natural Science Specializing in Chemistry

Iron Catalyzed C-C Coupling Reactions
Mechanistic Investigations

Anna Hedström

Cover picture: phenyl Fe(I), with two coordinating dimethyl ethers.
Graphics created with Molecule 2.1.

ISBN: 978-91-628-8686-8
Available online at: http://dhl.handle.net/2077/32608

Department of Chemistry and Molecular Biology
University of Gothenburg
SE-412 96 Göteborg
Sweden
Printed by Ineko AB
Kållered, 2013

Allting är svårt innan det blir enkelt

Johann Wolfgang von Goethe

Abstract

The mechanism of the iron catalyzed cross coupling of aryl electrophiles with alkyl Grignard reagents was studied. The reaction proceeds via a rate-limiting oxidative addition of the aryl halide to an Fe(I) complex generated *in situ*. A transmetalation from an aryl Grignard reagent occurs either before or after the oxidative addition. An exergonic reductive elimination closes the cycle, yielding the cross coupled product and regenerates the Fe(I) from Fe(III). Added ligands and dilution increases the stability of the active catalyst. The reaction can take place at dry ice temperature. Initial rate studies indicated that high concentrations of any reagent can lead to complete or partial catalyst deactivation. Under strongly reducing conditions, iron seems to form less active complexes that only slowly re-enter the catalytic cycle.

The iron catalyzed cross coupling of alkyl electrophiles with aryl Grignard reagents follows the same mechanism as the aryl electrophile – alkyl Grignard coupling. With the more weakly reducing aryl Grignard reagent, the iron catalyst is stable in diethyl ether without additives. The nature of the active catalyst has been under debate. In the couplings with aryl Grignard reagents, the active catalyst is an Fe(I) species. Fe(I) complexes are stable in ether, and they are active catalysts. The active iron catalyst has a spin state of S=3/2, even though the precatalytic Fe(III) salts have a high spin state (S=5/2). The spin change occurs after the first transmetalation, when the strong ligand field of the aryl group raises the energy of one d-orbital, inducing an electron pairing event.

Keywords: iron, homogenous catalysis, cross coupling, C-C bond formation, reaction mechanisms, kinetic investigations, competitive Hammett study, density functional theory

ISBN: 978-91-628-8686-8

List of publications

This thesis is based on the following papers, which are referred to in the text by their Roman numerals. Reprints were made with permission from the publishers.

I. **Mechanistic Investigation of Iron-Catalyzed Coupling Reactions**
J. Kleimark, A. Hedström, P.-F. Larsson, C. Johansson, P.-O. Norrby
ChemCatChem, **2009**, *1*, 152-161.

II. **Low Temperature Studies of Iron Catalyzed Cross Coupling of Alkyl Grignards with Aryl Electrophiles**
J. Kleimark, P.-F. Larsson, P. Emamy, A. Hedström, P.-O. Norrby
Adv. Synth. Catal. **2012**, *354*, 448-456.

III. **Iron-Catalyzed Coupling of Aryl Grignard Reagents with Alkyl Halides: A Competitive Hammett Study**
A. Hedström, U. Bollmann, J. Bravidor, P.-O. Norrby
Chem. Eur. J. **2011**, *17*, 11991-11993.

IV. **On the oxidation state of iron in iron-mediated C-C couplings**
A. Hedström, E. Lindstedt, P.-O. Norrby
Accepted for publication in *J. Organomet. Chem.*

Publications not included in this thesis:

a. **Diisopropyl(N,N,N',N'-tetramethylethylenediamine)zinc(II), the first crystal structure of a diisopropylzinc complex**
A. Lennartson, A. Hedström, M. Håkansson, *Acta Cryst.*, **2007**, E63(1), m123-m125.

b. **Toward total spontaneous resolution of sec-butylzinc complexes**

A. Lennartson, A. Hedström, M. Håkansson, *Organometallics* **2010**, *29*, 177-183.

c. **Assembly of Ethylzincate Compounds into Supramolecular Structures**

A. Hedström and A. Lennartson, *J. Organomet. Chem.* **2011**, *696*(*10*), 2269-2273.

Contribution to publications

Paper I. Contributed to the outline of the study. Performed a large part of the experimental work. Contributed to the interpretation of the results. Wrote parts of the manuscript.

Paper II. Contributed to the outline of the study. Contributed to the interpretation of the results. Wrote parts of the manuscript.

Paper III. Outlined the study. Performed all experiments and analyses. Contributed to the interpretation of the results. Wrote a large part of the manuscript.

Paper IV. Outlined the study. Performed all computational work and supervised the experimental work. Contributed to the interpretation of the results. Wrote a large part of the manuscript.

Abbreviations

acac	acetylacetonate
cat	catalyst
C-C	carbon-carbon
Cp	cyclopentadienyl
CyHexBr	cyclohexyl bromide
DEE	diethyl ether
DFT	density functional theory
EDG	electron donating group
EPR	Electron Paramagnetic Resonance
EWG	electron withdrawing group
GC	gas chromatography
I.S.	internal standard
IUPAC	International Union of Pure and Applied Chemistry
m-	meta-
NMP	N-methyl-2-pyrrolidone
OA	oxidative addition
Oct	octyl
OTf	trifluoromethanesulfonate
p-	para-
PBF	Poisson-Boltzmann Finite continuum model
PCM	Polarizable Continuum Model
Ph	phenyl
RE	reductive elimination
s	solvent
SET	single electron transfer
sol	solvent
THF	tetrahydrofuran
TM	transmetalation
TMEDA	*N*,*N*,*N*′,*N*′-tetramethylethylenediamine
WFT	wavefunction theory

Table of contents

1. Introduction

Life is chemistry: chemical reactions in our body, everyday chemicals, food preservatives, pharmaceuticals, fertilizers for our crops, large-scale industrial processes. Life as we know it would not be possible without chemistry.

Today the chemical society faces a challenging task: to make the most out of the worlds finite resources. It is our responsibility to develop green chemistry – we have to decrease waste production, conserve energy, reduce or eliminate generation of hazardous substances, find alternatives to precious metals, use catalysts and strive for high atom efficiency.

C-C bond forming reactions are amongst the most important reactions in organic chemistry. During the last decades the palladium catalyzed cross coupling reactions are the most prominent, and a basic tool in total synthesis. It is also applied widely in medicinal and process chemistry.[1] Despite their high utility, there are some drawbacks: palladium and the necessary ligands are expensive, palladium compounds are toxic and leaching of the palladium catalyst into final products can be problematic.

This thesis will give insight into iron catalyzed C-C coupling reactions, which have the potential to be sustainable, green alternatives to the highly utilized palladium (and nickel) catalyzed reactions. Mechanistic investigations will be undertaken to gain knowledge about the reactions, and the results will hopefully contribute to further development of new reaction protocols.

2. Transition metal catalysis

The first catalytic reaction described in the literature was the acid catalyzed Fischer ester synthesis, by C. W. Scheele.[2] The concept of catalysis was introduced by J. J. Berzelius in his annual report on the status of chemistry in 1835, and redefined by F. W. Ostwald in 1894, in connection with his studies of chemical kinetics.[3]

A catalyst is a species that increases the rate of a reaction, without itself being consumed. A catalyst primarily lowers the energies of the transition states. For the reactants and products, the energy changes are generally smaller. Because of the lower energy barrier, the catalyst has increased the rate of the reaction. In transition metal catalyzed reactions, adding the catalyst creates a new reaction pathway: more steps are required in the catalyzed reaction, but overall the barrier is lower than for the un-catalyzed reaction (Figure 1).

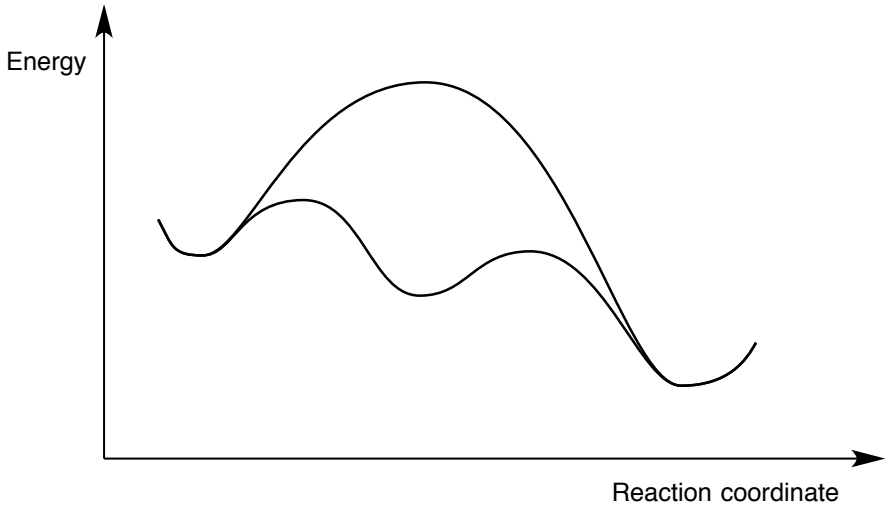

Figure 1. The catalyst has opened an alternative reaction path, with lower energy barrier.

A catalytic process is often depicted as a catalytic cycle; the catalyst is regenerated in the cycle, reactants are consumed and products are formed. In Figure 2, the starting point is a *catalyst precursor* (also called precatalyst): the precursor must be transformed into the *active catalyst* before entering the catalytic cycle. This is the case in many organometallic reactions, and can be due to the fact that the precatalyst is much easier to handle, more stable and/or cheaper than the active

catalyst. The activation of the precatalyst can inhibit the catalytic efficiency, if it is slow to enter the cycle or only a small part is activated.

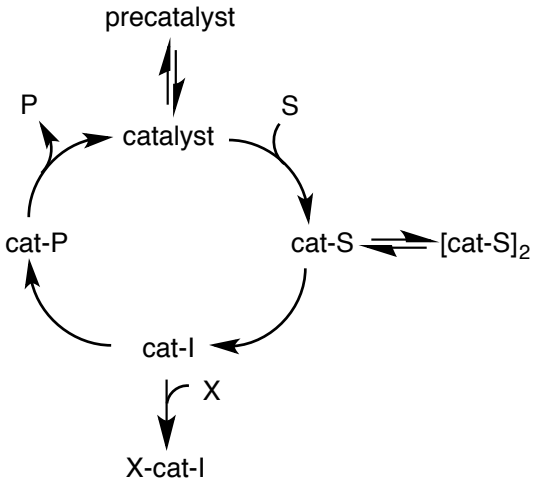

Figure 2. Catalytic cycle. S = substrate, I = intermediate, P = product, X = inhibitor

During the catalytic cycle, catalyst deactivation can occur. Species in the cycle may dimerize ($[cat\text{-}S]_2$), or ligands may detach/attach to create inactive compounds (X-cat-I). There are also additives that can facilitate the reaction by increasing the rate or selectivity – called *cocatalysts* (or *promotors*).[4]

Transition metal catalyzed reactions are among the most important in organic synthesis - a few examples are given below but an extensive overview is beyond the scope of this thesis.[5] IUPAC defines a transition metal as "an element whose atom has an incomplete d sub-shell, or which can give rise to cations with an incomplete d sub-shell."[6] The transition metals have between 1 and 10 *d*-electrons - often the metal can adopt multiple oxidation states, and coordinate a wide variety of ligands. These characteristics make transition metals ideal as catalysts in reactions: they can participate in redox reactions, switching reversibly between oxidation states and they may form labile intermediates necessary for an efficient catalytic process.

One example of a transition metal catalyzed reaction utilized in industry is the Monsanto acetic acid process, presented in Figure 3. Acetic acid is produced by carbonylation of methanol; the catalyst is a rhodium complex, and the selectivity is >99 %.[7]

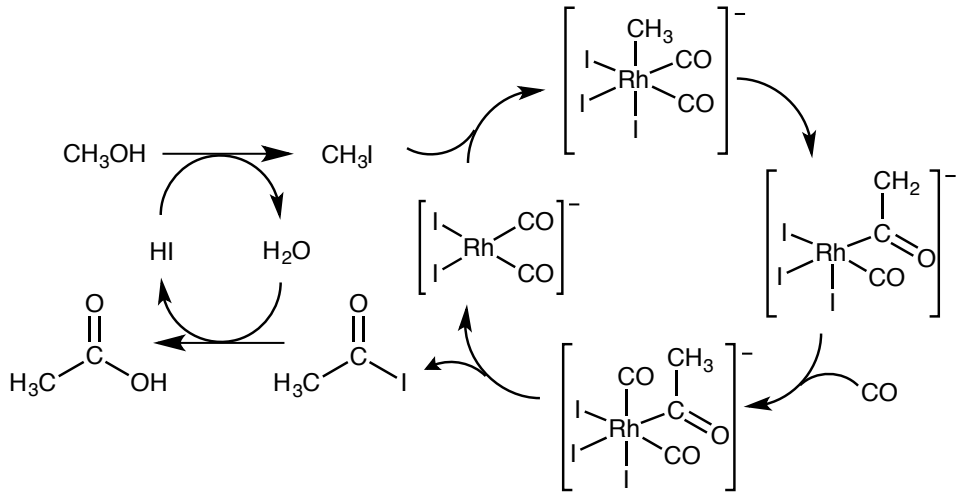

Figure 3. Proposed catalytic cycle for the Monsanto process.

The mechanism includes two connected cycles. Methanol is converted *in situ* to methyl iodide by HI. The generated methyl iodide oxidatively adds to the active rhodium catalyst. Carbon monoxide can then coordinate and insert, and the acetyl rhodium-complex can undergo reductive elimination to yield acetyl iodide and regenerate the catalyst. The acetyl iodide is hydrolyzed to acetic acid and HI. The oxidative addition and reductive elimination steps are two-electron processes typical for transition metal catalyzed reactions.

In organic synthesis, the impact of palladium and nickel catalyzed cross coupling reactions can hardly be overstated. They are applied in the synthesis of numerous natural products and biologically active compounds. One of the first catalytic cross coupling reaction, the Kumada coupling, where a Grignard reagent is coupled to an organic halide in the presence of nickel or palladium salts, was reported independently by both the groups of Kumada[8] and Corriu[9] in 1972. Since then the field has expanded, and resulted in several new coupling reactions such as Suzuki, Stille and Negishi coupling (see Scheme 1). Three of the most prominent researchers in the field, R. Heck, E. Negishi and A. Suzuki, were awarded the Nobel prize in 2010.[10]

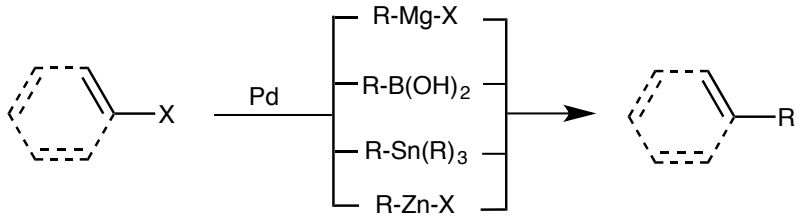

Scheme 1. A selection of catalytic cross coupling reactions, from top to bottom; Kumada, Suzuki, Stille and Negishi.

3. Mechanistic studies

A mechanism describes both *how* and *why* a reaction takes place. Mechanistic studies are important because they help us rationalize and simplify. It can be useful in predicting the outcome and course for new reaction types, and also help us modify and improve already known reactions.

3.1. Kinetic investigations

3.1.1. The rates of reactions

For the general reaction

$$a\mathrm{A} + b\mathrm{B} \ldots \rightarrow m\mathrm{M} + n\mathrm{N} \ldots \tag{1.1}$$

the reaction rate and the rate of disappearance of the reactants or the rate of formation of the products are related by

$$v = -\frac{1}{a}\frac{\mathrm{d[A]}}{\mathrm{d}t} = -\frac{1}{b}\frac{\mathrm{d[B]}}{\mathrm{d}t} = \frac{1}{m}\frac{\mathrm{d[M]}}{\mathrm{d}t} = \frac{1}{n}\frac{\mathrm{d[N]}}{\mathrm{d}t} \tag{1.2}$$

where v is the reaction rate. The rate law is the experimentally determined dependence of the reaction rate on reagent or product concentrations (or pressures of reagents/products in gas-phase reactions), and the general equation is written as follows

$$v = k[A]^x[B]^y \tag{1.3}$$

where the coefficient k is the rate constant for the reaction. k is dependent on the temperature, but independent of the concentration of the reactants. The powers to which the concentrations of reactants/products are raised (here: x or y) are determined experimentally from kinetic studies, and do not have to reflect the

stoichiometry of the reaction. The sum of x and y gives the order of the rate law – if $x = 0$ and $y = 1$, the order in A is 0, the order in B is 1, and the overall order is 1. Sometimes the order can be quite complex, and is more easily described with respect to each reagent. For example, the dimerization in Figure 2, which causes catalyst deactivation would result in a fractional order, and if any species acted as the inhibitor X we would get an inverse reaction order.

3.1.2. Determination of rate law

The determination of a rate law can be done by the *isolation method*, where the concentration of one species is varied, while the other reagents are present in large excess. Consider the reaction with the true rate law $v = k[A][B]$. If B is in large excess, the concentration $[B]_0$ will remain constant during the reaction and the rate law can be simplified to $v = k'[A]$, where the apparent rate constant $k' = k[B]_0$. The reaction has been transformed to a first-order form: it is described by a *pseudo-first order* rate law. By varying different species and having the others in excess, the order of each reactant can be determined – and so the overall rate law.

The *initial rate method* is a convenient way to avoid the need for an integrated rate law or pseudo-first order conditions. The rate is measured during the beginning of the reaction for several different initial concentrations of reactants. The assumption is that for the first ~10% of the reaction, the concentrations are virtually constant. It is crucial that the data sampling starts soon after the mixing of reactants. The initial rate method works well for slow reactions (preferably a half-time of >10 seconds).[11] For fast reactions, *stopped-flow technique* may be applied.[6]

3.1.3. Integrated rate laws

Rate laws are differential equations, and must be integrated to give the concentrations as a function of time. For each integrated rate law, there is a characteristic plot that will give a straight line, with the slope corresponding to the rate constant. The first order rate law for the disappearance of reactant A is written below.

$$-\frac{\mathrm{d[A]}}{\mathrm{d}t} = k_1[A] \quad (1.4)$$

Integration of (1.4) gives the integrated rate law, equation 1.5.

$$\ln\frac{[\mathrm{A}]_0}{[\mathrm{A}]} = k_1 t \quad (1.5)$$

If $\ln([A]_0/[A])$ is plotted against t, then a first-order reaction gives a straight line through the origin, with slope k_1.

3.1.4. The Hammett equation

Described already in 1937,[12] the Hammett equation (1.6) is one of the most common linear free energy relationships:

$$\log\left(\frac{k_X}{k_H}\right) = \rho\sigma \quad (1.6)$$

The equation describes the influence of meta- or para-substituents X on the reactivity of the reaction center Y in benzene-derivatives (*m*-X-Ph-Y or *p*-X-Ph-Y). k_X is the rate constant* for the reaction with the substituted benzene-derivative and k_H is the rate constant for the corresponding un-substituted substrate (H-Ph-Y). The substituent constant σ describes how electron donating (negative σ) or withdrawing (positive σ) the substituent is relative the H. The constant is based on the difference between pK_a of suitably substituted benzoic acid derivatives. There are also related electronic substituents constants (σ+, σ-, σ•) based on other reactions, mostly applicable to special cases when the substituent is in direct conjugation with a charge or a radical.[13] The reaction constant ρ is a measure of how susceptible the rate constant is to changes in the substituent group. Reactions with a positive ρ are accelerated by substituents with positive σ: the electrons are

* The equation can also be used for equilibrium constants, $\log\left(\frac{K_X}{K_H}\right) = \rho\sigma$

drawn away from the aromatic ring, and a negative charge build-up in the transition state is stabilized.

3.1.5. Competitive Hammett studies

As described above, the sign and magnitude of ρ provide information about what happens in the rate-determining step. Measuring the rate constants k_X and k_H accurately is not always possible – the use of a competition experiment can simplify the experimental procedure and provide other valuable information. A competitive Hammett study (see Figure 4) gives information about the *selectivity-determining* step, whereas a normal Hammett study always measure the *rate-determining* step. These steps do not necessarily coincide.

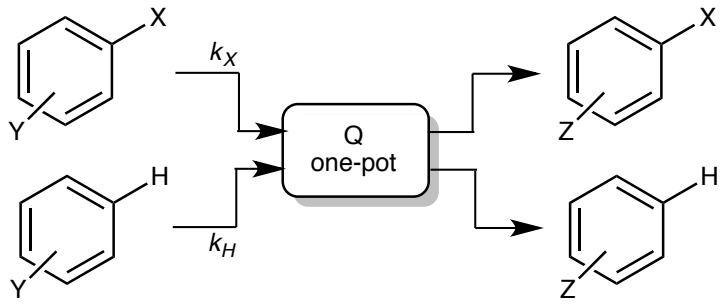

Figure 4. Hammett competition experiment, where Q is a general reagent.

The reaction can be followed either by monitoring substrate disappearance or product formation (if no significant side-reactions occurs). If the kinetic dependence on all reagents is assumed to be the same for the competing substrates, the rate expressions can be written as shown in equation 1.7 and 1.8.

$$-\frac{\mathrm{d[X]}}{\mathrm{d}t} = k_x[Q]^q[X] \tag{1.7}$$

$$-\frac{\mathrm{d[H]}}{\mathrm{d}t} = k_H[Q]^q[H] \tag{1.8}$$

Dividing equation 1.8 with 1.7 cancels out all terms that are identical for both reactions, and yields the simple equation 1.9.

$$\frac{\mathrm{d[X]}}{\mathrm{[X]}} = \frac{k_X}{k_H}\frac{\mathrm{d[H]}}{\mathrm{[H]}} \tag{1.9}$$

The time dependent terms are no longer included in 1.9. Integrating equation 1.9 gives equation 1.10, where only the initial concentrations ($[X]_0$ and $[H]_0$, respectively) and concentrations of the substrates need to be experimentally determined to deduce the relative rate constant, k_{rel}.

$$\ln\frac{[X]_0}{[X]} = \frac{k_X}{k_H}\ln\frac{[H]_0}{[H]} \text{ , where } \frac{k_X}{k_H} = k_{rel} \tag{1.10}$$

Equation 1.10 can be used for any two points, but is more accurate when used as a straight line without intercept. The relative rate constant is then used to construct the competitive Hammett plot from the equation 1.11.[14]

$$\log(k_{rel}) = \rho\sigma \tag{1.11}$$

The simplicity of competition experiments make them very useful – and combined with computational methods, a powerful tool in mechanistic investigations.

3.2. Computational approaches

The use of molecular modeling in mechanistic investigations has seen an explosive growth in recent years. This is due to the combination of more powerful computers and development of efficient methods based on density functional theory (DFT). In DFT, the Schrödinger equation is not solved directly – instead it solves a less exact equation based on the electron density. The accuracy achieved by using DFT instead of methods based directly on the Schrödinger equation (fundamental wavefunction theory, WFT) is significantly higher with the same set of computational resources.[15] The most successful methods utilize a mixture of DFT and WFT,[16] where the hybrid functional B3LYP[17] is the most popular member.

Like all quantum mechanical methods, B3LYP and other hybrid DFT methods deliver potential energies *in vacuo* (sometimes called *gas phase*). Most organic reactions are carried out in solvent and although the potential energies *in vacuo* hold a lot of information, comparison with experimental energies require determination of free energies in solvent. The most important factors here include vibrational corrections to enthalpy and entropy, and interaction with solvent molecules. The influence of solvent can be approximated by *continuum models*, like PCM (Polarizable Continuum Model).[18] In the current work we use a closely related method, PBF (Poisson-Boltzmann Finite continuum model).[19] The continuum solvent models do not capture bonding interaction, so explicit solvent molecules may be added to the complex in the calculation.

In recent years several improvements have been made in the DFT field. One of the more significant changes has been to include a correction for *London dispersion forces* (instantaneous dipole – induced dipole forces), known to be absent from standard DFT methods. The dispersion interaction is generally insignificant for small model systems, but for realistic calculations of actual experimental systems, the impact can be huge. In this work, we have used the recently developed empirical D3-correction from Grimme.[20]

4. Iron complexes

Iron is the fourth most abundant element in earth's crust. It exists in a wide range of oxidation states, the most common being +III and +II. Usually, if a Fe(II)-salt is exposed to air for a longer period of time, it will oxidize to Fe(III), but some Fe(II) complexes with strong ligand fields are unusually stable (e.g. ferrocene, potassium hexacyanoferrate(II)). Fe(II) complexes prefer an octahedral coordination sphere, as do Fe(III). Fe(0) coordinates five or six electron-accepting ligands with trigonal bipyramidal or octahedral geometry, respectively, and Fe(-II) is usually tetrahedral.[21] A few examples of complexes are represented in Figure 5.

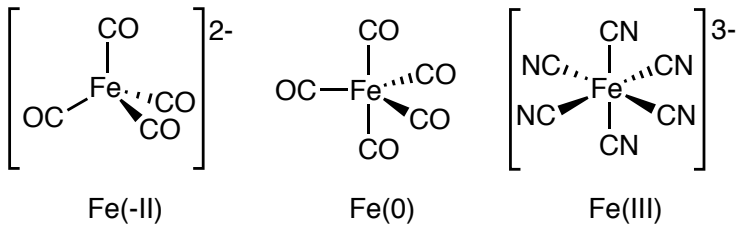

Figure 5. A display of different geometries iron complexes can adapt. From left to right: Collman's reagent, pentacarbonyl iron and hexacyanoferrate.

By switching to low field ligands such as chloride, the coordination sphere and spin state of iron can be altered (see Figure 6) making iron a very versatile transition metal.

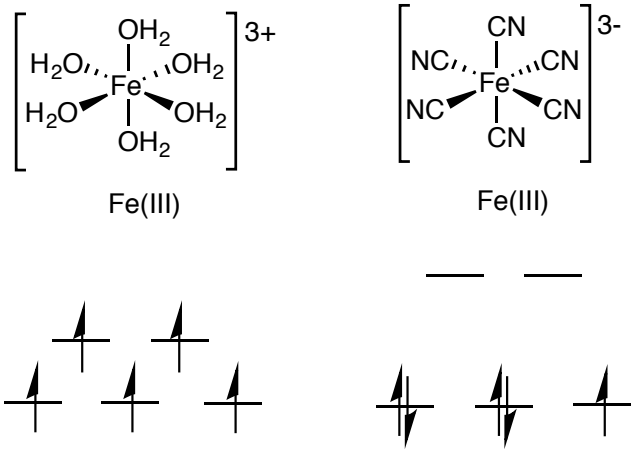

Figure 6. Iron(III) as hexaaqua and hexacyano complexes; water is a weak field ligand, making the hexaaqua complex a high spin complex; cyanide is a strong field ligand, resulting in a low spin complex.

Some metal complexes may also change spin states when subjected to different temperature, magnetic fields or light irradiation; a so-called *spin crossover* (or *spin transition*) takes place. In Figure 7, an Fe(II) complex is cooled down and the spin state goes from high spin to low spin.[22]

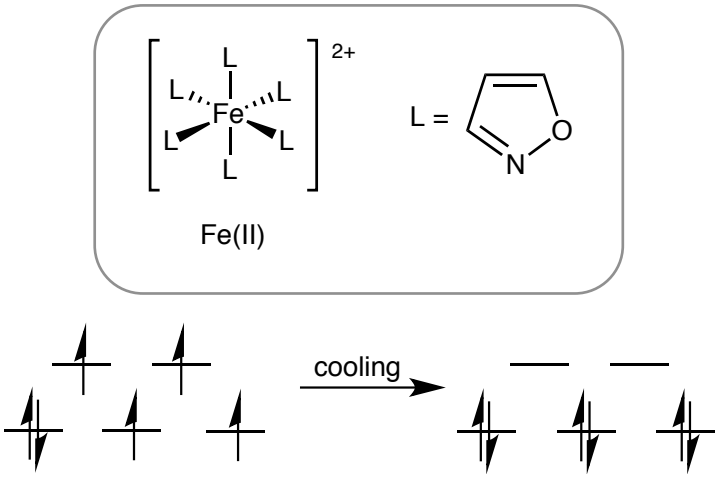

Figure 7. Spin crossover in an octahedral Fe(II) complex.

5. Iron catalyzed C-C coupling

Due to its abundance in nature and its ability to adopt several different oxidation states, iron is present in multiple biological processes. It is the active center in many metalloenzymes that catalyze redox reactions or participate in electron transfer. Iron is also used in oxygen transport, hydroxylations, monooxygenations and much more.[23]

The industrial Haber-Bosch process, where ammonia is synthesized from hydrogen and nitrogen under high-pressure and high temperature, is considered to be one of the most important inventions of the 20th century. The process made nitrogen fixation economically feasible, and it is estimated that *ca.* 40 % of the world's population is sustained by fertilizers from ammonia synthesized through the Haber-Bosch process.[24] The reaction is catalyzed by iron, usually in combination with oxides of other metals.

In organic chemistry, iron can be used to mediate and catalyze a multitude of different reactions: addition reactions, substitution reactions, cycloadditions, hydrogenations, rearrangement, polymerizations, cross coupling reactions and more.[21, 25] In this thesis, the focus will be on iron catalyzed C-C coupling reactions.

5.1. The Kharasch-Grignard reaction

In 1941 Kharasch and Fields studied the effect of different metallic halides on the reaction of aryl Grignard reagents in the presence of organic halides.[26] Previously, the reaction in Scheme 2 without addition of organic halides had been investigated with yields ranging from 25-100 % for different salts.[27]

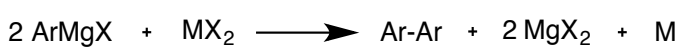

Scheme 2. Metal-mediated homocoupling reaction.

They stated that aryl magnesium halide reacted in the presence of metallic halide to give biaryl in agreement with earlier findings by Gilman and Lichtenwalter.[27a]

When they added an aryl halide to a mixture of Grignard reagent and a small amount of metallic halide, a vigorous reaction took place (Scheme 3). The aryl halide acted as an oxidizing agent, and a good yield of biaryl could be obtained (5 mol% of $FeCl_3$ yielded 74 % of biphenyl). They also proved that the aryl group in the biaryl came exclusively from the aryl Grignard reagent.

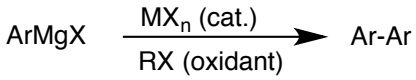

Scheme 3. The Kharasch-Grignard reaction

The study was extended to include a variety of Grignard reagents and alkyl halides, where the Grignards were coupled under mild conditions by catalytic amounts of transition metal salts.[28] The reaction known as *the Kharasch-Grignard reaction* or simply *the Kharasch reaction* during the 1940's to the 1970's was subjected to extensive mechanistic investigations by several groups. Abraham and Hogarth present an overview of the different mechanistic suggestions.[29] The early studies gave somewhat contradictory results, and the complexity of the reaction became evident. Kharasch and Fields suggested a heterogeneous radical mechanism for the aryl Grignard homocoupling, where a free aryl radical is formed on the surface of a metal "subhalide".[26] Tsutsui proposed formation of a diphenyl metal intermediate that decomposes to biphenyl via a "π-radical hybrid".[30] Parker and Noller looked into the cobalt or copper-catalyzed alkyl Grignard – alkyl halide coupling, and drew the conclusion that the reaction can proceed via two pathways; one with the formation of a free radical intermediate, and the other with formation of catalyst complex containing both Grignard reagent and alkyl halide without formation of free radicals.[31]

Iron did not play the leading part in the studies of the Kharasch reaction until 1971, when Kochi and Tamura published their paper "*Iron catalysis in the reaction of Grignard reagents with alkyl halides*".[32]

5.2. Iron catalyzed cross coupling

In the 1970's Kochi published several articles on the subject of iron catalyzed coupling of Grignard reagents with organic halides (Scheme 4), which he referred to as the Kharasch reaction.[33]

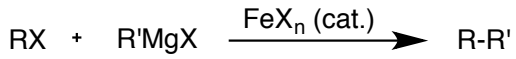

Scheme 4. Iron catalyzed cross coupling

Mechanistic studies were undertaken and Kochi proposed an Fe(I)-Fe(III) catalytic cycle (Figure 8) based on the mechanism of the Kumada coupling,[8, 9] which was "*intended to form a basis for discussion and further study of the catalytic mechanism* […] *oxidation numbers are included only as a device for electron accounting and are not necessarily intended to denote actual changes in oxidation state*".[33e]

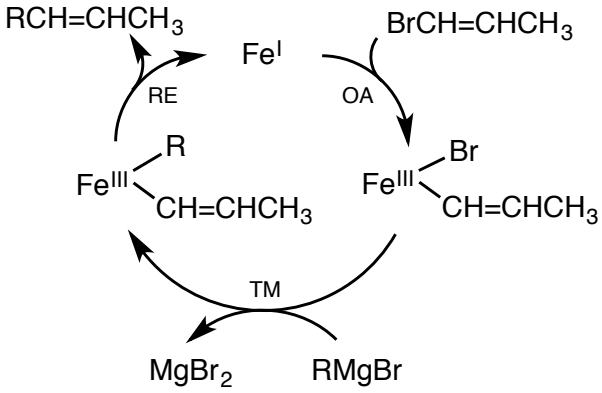

Figure 8. Proposed catalytic cycle with oxidative addition (OA), transmetalation (TM) and reductive elimination (RE).

The oxidative addition was found to be the rate-limiting step and E/Z stereospecific. There where side reactions, which could be accounted for by multiple exchanges and disproportionation from organoiron(III) intermediates. Different ferric salts where used as precatalysts, and by looking at the byproduct profile, Kochi drew the conclusion that Fe(III) was likely reduced to Fe(I) by Grignard reagent (but Fe(0) could not be excluded). Aggregation of the catalytically active iron species could be responsible for the deactivation when the catalyst was allowed to stand for prolonged times.

5.2.1 Revival of the iron catalyzed cross coupling

After Kochi's extensive mechanistic work, the iron catalyzed cross coupling was overshadowed by the palladium and nickel catalyzed reactions for many years, mainly due to byproduct formation and the requirement of a large excess of the vinyl halide. There were only a few publications on the subject during the 80's and 90's.[34] In 1998, Cahiez *et al.* used different co-solvents in the iron catalyzed alkenylation of organomagnesium compounds (Scheme 5).[35]

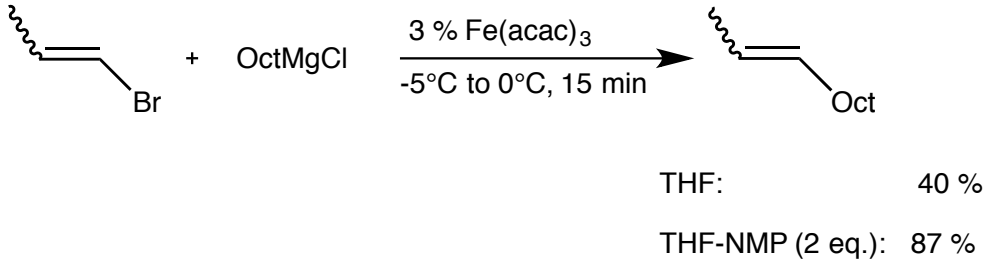

Scheme 5. Iron catalyzed alkenylation of Grignard reagents by Cahiez *et al.*

The increase in yield and stereospecificity was impressive, especially with *N*-methylpyrrolidone (NMP). Even alkenyl chlorides, which are considered to have low reactivity in these reactions, could be coupled in good yields (though more NMP was needed, 9 equivalents). The role of NMP is likely as a stabilizing ligand for the catalytic active iron species. The reaction tolerates functional groups such as bromides, esters, amides and ketones. With the important contribution from Cahiez, the iron catalyzed cross coupling reaction could now compete with the Pd or Ni catalyzed analogs in preparative organic chemistry.

Fürstner and coworkers opened up the field further in their paper "*Iron-Catalyzed Cross-Coupling Reactions*" in 2002, with catalyst optimization, screening of substrate scope, applications in total synthesis and mechanistic studies.[36] They pointed out that the growing amount of accessible functionalized Grignard reagents will play an important part in the future of iron catalyzed coupling reactions.[37]

5.2.2 Scope of iron catalyzed cross coupling

Iron catalyzed cross coupling seems to allow all possible combinations of sp^2 and sp^3 nucleophiles and electrophiles (Figure 9), though some require special conditions and only give moderate yields.[38] In chapter 7, the results from studies of the sp^2-sp^3 and sp^3-sp^2 couplings will be presented and discussed.

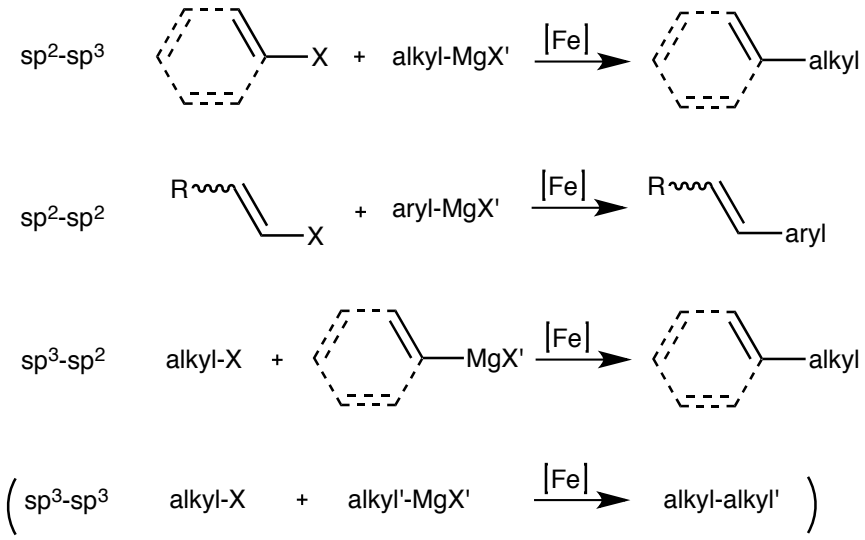

Figure 9. Combinations of sp^2 and sp^3 in iron catalyzed cross coupling. For aryl-aryl (instead of alkenyl – aryl), coupling is possible under certain conditions.[38b-d]

5.2.3. Suggested mechanisms

The iron catalyzed cross coupling between organic halides and Grignard reagents has been the target reaction for several mechanistic investigations.[38, 39] The most popular mechanism is based on the nickel and palladium catalyzed Kumada-Tamao-Corriu reaction, with oxidative addition (OA), transmetalation (TM), followed by reductive elimination (RE).[4a] If the OA or TM occurs first is unknown, and both pathways must be taken into account (depicted in Figure 10).

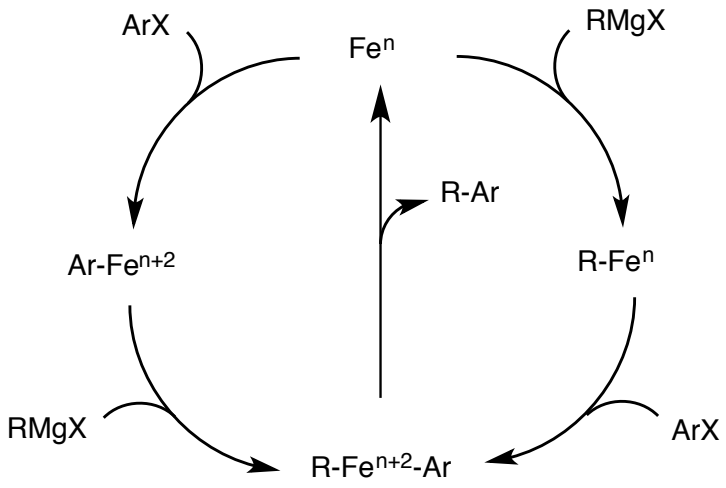

Figure 10. Two possible pathways for the iron analog of the Kumada-Tamao-Corriu reaction. Ligands are excluded.

Another mechanism to consider is cross coupling via a radical pathway similar to the above mechanism, where the catalyst reacts with an alkyl halide by single electron transfer (Figure 11).[40]

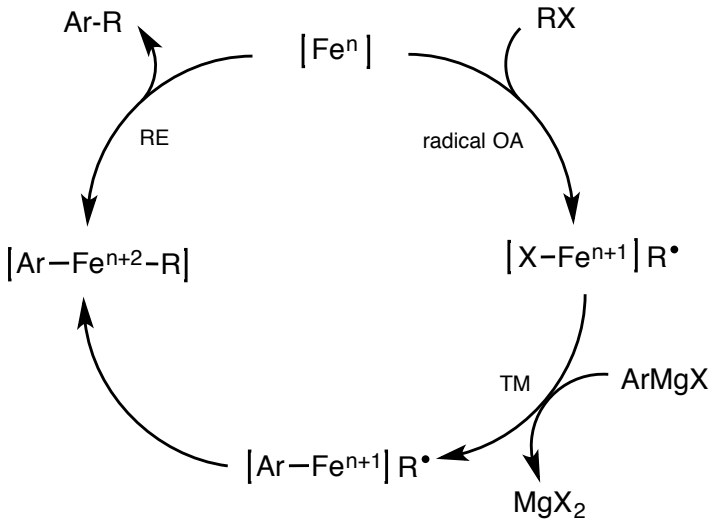

Figure 11. Cross coupling via a radical pathway.

5.3. Oxidation state of iron in the catalyst

Currently, there are mainly two proposed oxidation states for the active iron catalyst in the catalytic cycle to consider: the low-valent Fe(-II) complex or the rare Fe(I) complex.[38a, g, 39, 41]

5.3.1. Fe(-II)

Low-valent Fe(-II) complexes have been used in cross coupling reactions with good results. They have been characterized by X-ray crystallography and used in both alkyl-aryl and aryl-alkyl cross coupling (Figure 12).[36, 42, 43]

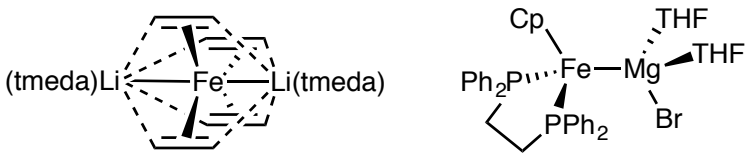

Figure 12. Examples of Fe(-II) complexes. The left complex has been used successfully in C-C cross coupling; the right one is an example of a "inorganic Grignard reagent".

The equally high yields obtained by using the Fe(-II) complex or the precatalysts Fe(III) or Fe(II) have been used as proof that Fe(-II) is the catalytically active oxidation state. The so-called "inorganic Grignard reagent", a highly reduced iron-magnesium cluster $[Fe(MgX)_2]_n$, is suspected to play a vital role in the catalytic cycle (see Scheme 6 for generation of the low-valent iron).[44]

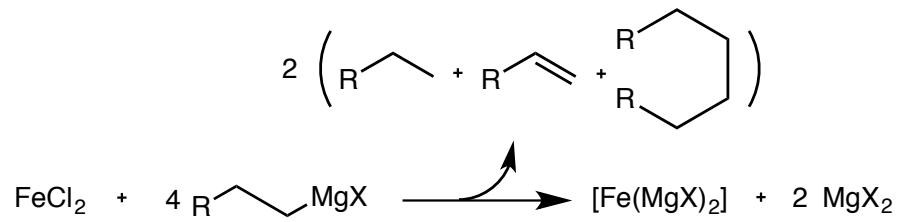

Scheme 6. Reduction of iron to inorganic Grignard reagent.

5.3.2. Fe(I)

Based on byproduct formation, Kochi and coworkers drew the conclusion that the active iron catalyst had the oxidation state +I, even though they could not isolate it.[32,33] EPR studies of the reduction of tris(dibenzoylmethido)iron(III) by Grignard reagent shows a signal centered around g = 2.08,[45] consistent with spectra of other paramagnetic Fe(I) complexes reported by Gargano and coworkers[46] and Muetterties *et al.*[47]

Recently Bedford *et al* successfully isolated catalytically active Fe(I) intermediates for iron catalyzed Negishi coupling (see Figure 13).[48] They investigated the reaction of an Fe(II) precatalyst with diaryl zinc and came to the conclusion that Fe(II) is reduced rapidly to Fe(I). Further reduction to oxidation states below +I is far too slow to be relevant in the catalytic cycle.

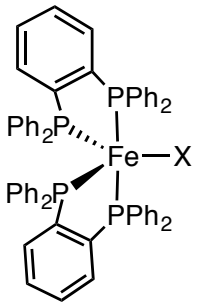

X = tolyl, Cl, Br

Figure 13. Fe(I) complexes structurally determined by Bedford *et al.*

EPR measurements of the complex together with DFT analysis of the aryl-Fe structure in the figure above were consistent with an Fe(I) low spin (S =1/2) complex. The group of Cárdenas studied iron catalyzed alkyl-alkyl cross coupling, and also reported evidence for Fe(I) complexes in the catalytic cycle.[38g]

6. Aim of the thesis

The overall goal of the studies performed in this thesis to expand the chemists "toolbox" to include more sustainable alternatives to the precious metal catalyzed C-C coupling reactions used today.

The main objective of this work is to gain a deeper understanding of iron catalyzed C-C coupling reactions; what are the intermediates, the catalytic active species? How do solvent, temperature, additives and other factors affect the reaction progress? Mechanistic studies are important, if not crucial, in designing and optimizing new and already known reactions. Both experimental and theoretical methods are applied in the mechanistic investigations included in this thesis.

7. Mechanistic investigations of iron C-C coupling

In this chapter the results from four papers will be presented and discussed. Paper I and II concern the iron catalyzed cross coupling of alkyl Grignard reagents and aryl halides. Both experimental and theoretical techniques were applied to elucidate the reaction mechanism. Paper III is a competitive Hammett study of aryl Grignard reagents and is preceded by a brief solvent screening. In Paper IV, stoichiometric homocoupling of aryl Grignard is studied experimentally and computationally to determine the oxidation state of the catalytically active iron complex.

7.1. *Paper I*: Mechanistic investigation of iron catalyzed coupling reactions

The mechanism of the iron catalyzed cross coupling of aryl electrophiles with alkyl Grignard reagents was studied by a combination of GC monitoring, Hammett competition experiments, and DFT calculations.

7.1.1. GC monitoring

There are many reactions that can occur when the Grignard reagent is added to the reaction mixture depicted in Scheme 7. We expect that the Grignard reagent will react quickly with the precatalytic iron salt and generate the active iron catalyst.

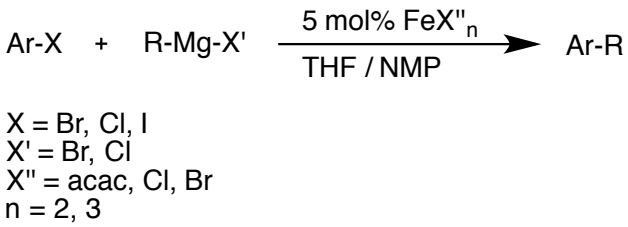

Scheme 7. General scheme for cross coupling of aryl halide and alkyl Grignard reagent.

First a transmetalation takes place, where an alkyl iron species is generated. From the alkyl iron, the reduction could occur by several pathways (Scheme 8). β-hydride elimination would yield an alkene and an iron-hydrido complex, which could undergo a base-assisted elimination (path a). The alkyl iron could also undergo a direct elimination (path b) – both paths produces alkene, alkane and a reduced iron species. If the alkyl iron is transmetalated once more, we get a dialkyl iron that can undergo an internal elimination (path c) or a reductive elimination (path d). The different pathways result in the byproducts alkane, alkene and the homocoupled product. Each path leads to reduction of iron; the starting iron complex has gained two electrons.

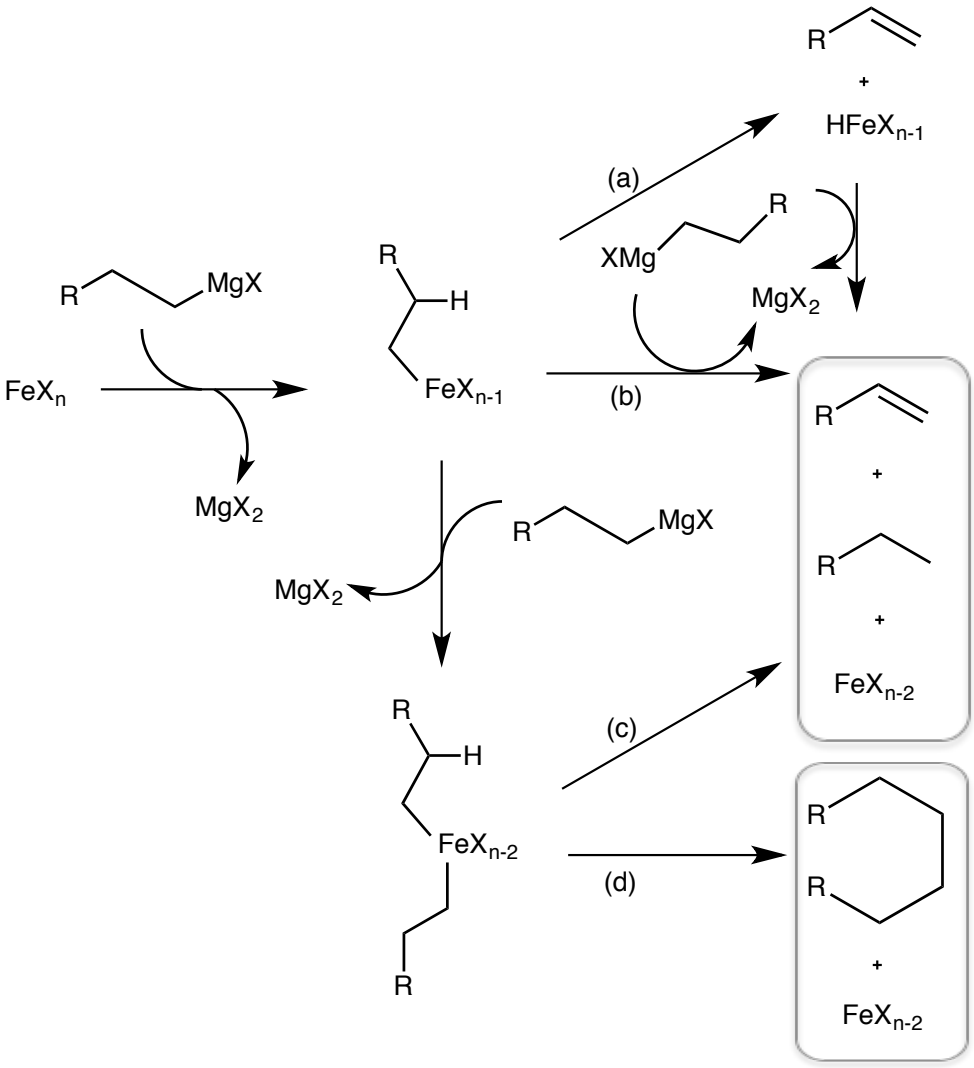

Scheme 8. Reduction of iron by several different pathways. See text for discussion of (a)-(d).

It should be possible to deduce the oxidation state of the reduced iron complex by keeping track of the amount of formed byproducts. The problem with the analysis is that additional alkane is formed during work-up of the reaction mixture (unreacted alkyl magnesium halide). Fortunately, the amount of alkane can be excluded from the analysis; all reactions that reduce iron also produce one equivalent of alkene or homocoupled product. Thus the total number of electrons added to iron can be calculated as twice the sum of alkene and homocoupling product.*

To further complicate the analysis, commercially available or synthesized Grignard reagent contains both alkane, alkene and homocoupled product. We designed a titration experiment, where it is possible to compensate for both contaminants and some fluctuations in experimental conditions (Scheme 9).

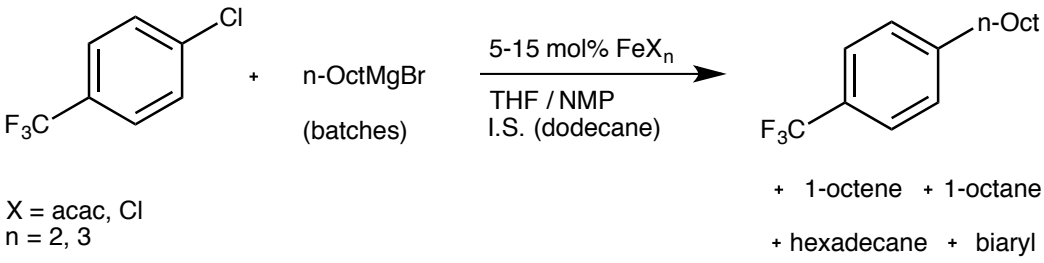

Scheme 9. Standard titration experiment, with the cross coupled product and potential byproducts. The Grignard reagent is added in small portions to the reaction mixture.

The iron salt was dissolved in tetrahydrofuran (THF) with NMP as co-solvent. The aryl chloride (or triflate in the competitive Hammett study, *vide infra*) was added, with dodecane used as internal standard. Small portions of Grignard reagent were added to the reaction flask, and the mixture was allowed to react for 5 minutes before a sample was quenched and analyzed by GC. The mass-balance of aryl was checked throughout the titration (constant value when small volumes of samples are withdrawn), as well as the amount of alkyl, which was steadily increasing proportional to added alkyl Grignard. All components where plotted

* Radical species may be present in the reaction mixture.[28, 33] If they are not trapped or react with for example solvent, they will recombine to form the products depicted in Scheme 8.

against the total amount of alkyl fragments (corresponding to the amount of added Grignard reagent). A typical plot is presented in Figure 14.

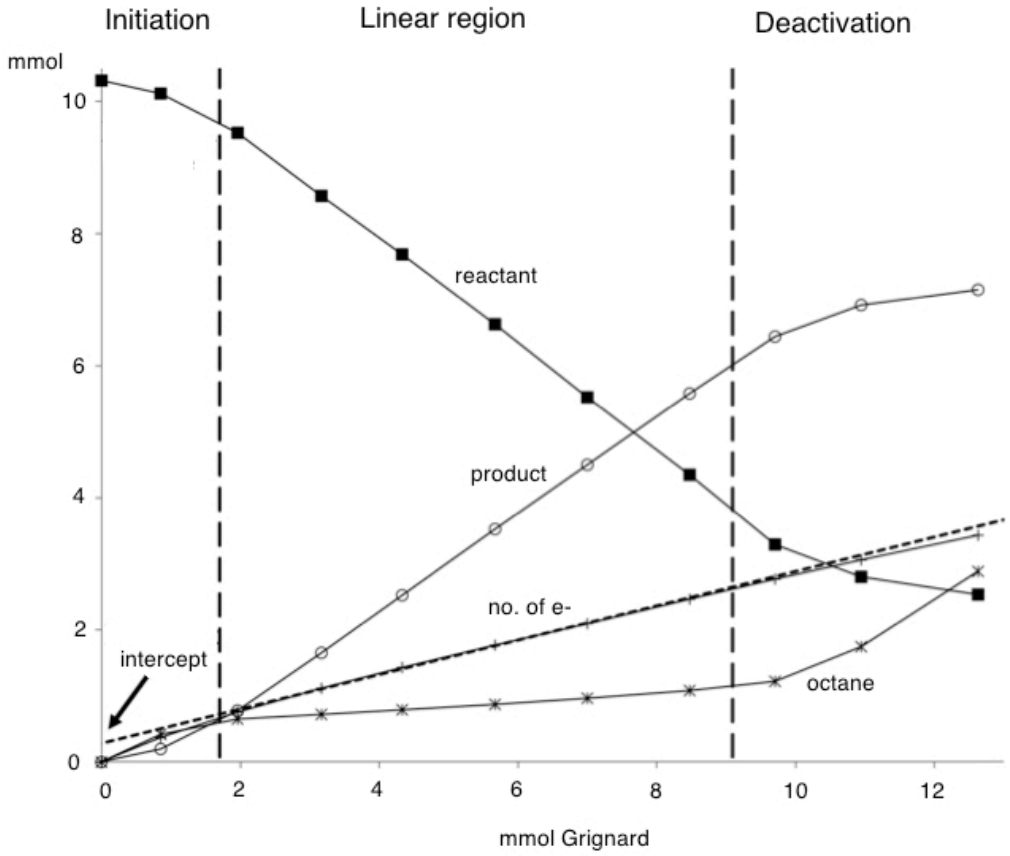

Figure 14. Representative plot from a titration experiment.

In the plot, we can see three distinct phases of the reaction. First, an initiation phase, where the Grignard reagent is consumed in the reduction of the iron salt to generate the active catalyst. The substrate (aryl halide) is unreacted during the initiation. When the active catalyst enters the reaction, the cross coupling takes place – this is the linear phase where the amount of cross coupled product is increasing linearly, and the substrate is decreasing proportionally. Suddenly, there is an increase in alkane formation; the reaction is in the deactivation phase. The product formation starts to decline and the Grignard reagent is not consumed (unreacted alkyl Grignard is protonated during the work-up and yields alkane).

As stated above, the number of electrons the precatalyst iron salt has gained can be calculated as twice the sum of alkene (here: octene) and

homocoupled product (here: hexadecane). The analysis is valid in the linear phase: to determine the linear region the F-test* was used for each experiment. Plotting the amount of alkene and homocoupled product times two would give a straight line with zero slope in the linear region, if the Grignard reagent did not already contain the possible oxidation products. Instead, we get a straight line with a positive slope. To retrieve the value of interest and compensate for contaminants, we extrapolate the slope of the oxidation products down to x=0, where the value of the intercept gives us the number of electrons added to iron. Dividing the y-intercept with the amount of iron salt for each experiment resulted in Table 1.

* The F-test is a statistical test mainly used on models where the data has been fitted using least squares. The test can be used to decide if the variables contribute with useful information, and thereby should be included in the data set.

Table 1. Number of electrons (e-) added to each iron atom, with standard regression error.

Entry	Iron salt	Fe [mol %]	THF [mL]	no. of e-/Fe
1	$FeCl_2$	5	35	0.256 ±0.004
2		10	35	0.146 ±0.004
3		15	35	0.237 ±0.006
4		5	70	0.566 ±0.007
5		5	105	0.699 ±0.067
6	$Fe(acac)_2$	5	35	0.684 ±0.001
7		10	35	0.705 ±0.01
8		15	35	0.695 ±0.013
9		5	70	0.809 ±0.01
10		5	105	0.736 ±0.063
11	$FeCl_3$	5	35	0.605 ±0.006
12		10	35	0.614 ±0.005
13		15	35	0.642 ±0.014
14		5	70	1.094 ±0.039
15		5	105	1.026 ±0.029
16	$Fe(acac)_3$	5	35	0.991 ±0.011
17		10	35	0.903 ±0.04
18		15	35	1.127 ±0.021
19		5	70	1.123 ±0.023
20		5	105	1.169 ±0.031

The results are somewhat surprising. For the ferrous salts, the number of electrons per iron ranged from 0.15 to 0.81, and for ferric salts from 0.61 to 1.17. It is not possible to reduce the iron salt by a fraction of an electron – something else is going on. Even when only 0.15 e- are used for the reduction (see entry 2, Table 1), the cross coupling reaction is effective. Apparently, not all of the available iron is reduced. We started to look for trends in the table. Diluting the reaction mixture by a factor two (for example entry 1 and 4, 14 mM iron vs. 7 mM) increased the e-/Fe ratio for the chloride salts. The acetylacetonate salts, $Fe(acac)_2$ and $Fe(acac)_3$ gave more consistent data than the chloride salts. If oligomers of iron are present in the reaction, dilution and having a bidentate ligand (like acetylacetonate) coordinated to iron would favor monomers. As a result, a larger fraction of iron would be available for reduction. The expected value for Fe(II) versus Fe(III) should differ with 1.0 electron – this is not the case here, another indication that only a fraction of the added iron is reduced and enters the catalytic cycle. The Fe(II/III) species present in solution would be expected to comproportionate rapidly with any low-valent iron complexes. The low values in Table 1 and the presence of Fe(II) and Fe(III) make the mechanistic proposal with a catalytically active Fe(-II) species (see section *5.3.1.*) highly unlikely.

The GC monitoring study gave no reliable evidence concerning the oxidation state of the active catalyst. However, the study yielded useful information about the reaction conditions. Dilution, addition of a bidentate ligand, high substrate concentration and slow addition of Grignard reagent can prevent catalyst deactivation. Taken together, these observations indicate that catalyst deactivation occurs primarily through precipitation of low-valent iron. In all titration experiments, significant amount of precipitate formed towards the end of the reaction.

7.1.2. Competitive Hammett study

A competitive Hammett study was set-up according to Scheme 10. Aryl triflates were chosen as substrates, due to the low reactivity of the aryl chlorides with electron-donating groups.[49]

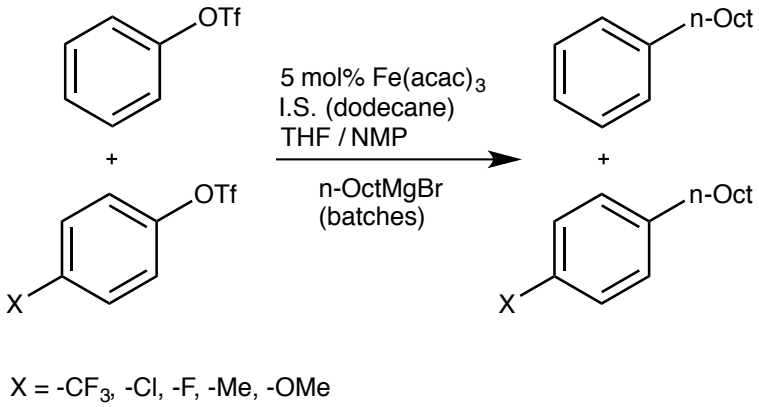

Scheme 10. Competitive Hammett study of aryl triflates.

The Grignard reagent was added in batches to the competing substrates and the disappearance of the substrates was monitored in the linear phase, *vide supra*. Assuming the same kinetic dependence on all reagents and catalysts for both substrates (substrate X, *p*-substituted phenyl triflate and substrate H, phenyl triflate) the relative rate, $k_{rel}=k_X/k_H$, was obtained by fitting the expression $\ln([X]_0/[X]) = k_{rel}\ln([H]_0/[H])$ for all points in the linear phase. The first point in the linear phase was taken as the initial concentration of substrate, $[X]_0$ and $[H]_0$ respectively. The relative rates for the different *p*-substituted phenyl triflates are presented in Table 2, along with literature σ-values for the substituents.[13]

Table 2. Relative rates obtained for the *p*-substituents.

p-substituent	k_{rel}	σ	σ−	σ•
OMe	0.32	-0.27	-0.26	0.24
Me	0.51	-0.17	-0.17	0.11
F	3.2	0.06	-0.03	-0.08
Cl	17.7	0.23	0.19	0.12
CF_3	165[a]	0.54	0.65	0.08

[a] Determined in competition with *p*-Cl substrate, $k(CF_3)/k(Cl)=9.34$.

The relative rates where fitted to the σ-values using the Hammett expression, $\log(k_X/k_H) = \rho\sigma_X$. As can be seen in Figure 15, the correlation is best with the normal σ, giving a large, positive slope: $\rho = +3.8$. There seems to be a systematic

error, with all the k_{rel}-values slightly above the added trendline. However, this does not affect the qualitative value of ρ.

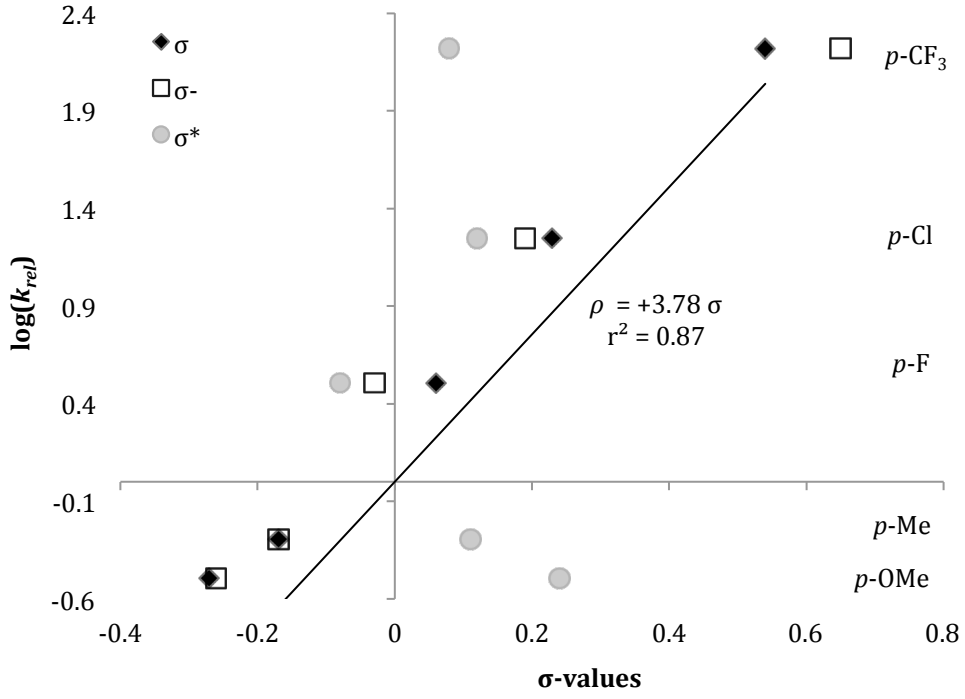

Figure 15. Hammett plot of log(k_{rel}) versus different σ's.

The reaction is very fast with electron-withdrawing (EWD) substituents; the relative rate for *p*-trifluoromethyl phenyl triflate had to be determined in competition with the *p*-chloro phenyl triflate. The high positive value of ρ indicates that the oxidative addition is an *effectively irreversible* step in the catalytic cycle. There is a negative charge build-up at the reaction center of the oxidative addition transition state. EWD substituents help to stabilize the charge in the transition state, lowering the reaction barrier and the reaction rate increases.

The oxidative addition could also take place via another mechanism: a single electron transfer (SET) could generate an aryl radical anion.[40] The anion can eliminate the leaving group and the resulting aryl radical could add to the metal. This mechanism would correlate well with a combination of σ^- and $\sigma^\bullet$, if the formation of aryl radical anion is rate-limiting. This is not in agreement with the results. For example, with the fluoro substituent, it would result in a decrease of

the rate; here a threefold acceleration is observed (see Table 2). Probably the generation of anion radicals is not selectivity-determining in this reaction.

The $\sigma^{\bullet}$ seldom gives good correlation by itself, usually a combination with other σ's is needed. Combining σ^{-} and $\sigma^{\bullet}$ gave a poor fit as stated above. σ^{+} and $\sigma^{\bullet}$ gave a much better fit, which can be explained by a partial donation of electron density from iron to the aryl group during the oxidative addition. This is supported by calculations (*vide infra*) showing a significant spin density on the aromatic carbons in the oxidative addition transition state.

7.1.3. Computational study

The experimental data, though informative, was inconclusive. A computational study was performed in the group* to shine some light on the mechanism. Density functional theory (DFT) was used to calculate the reaction free energy for all single steps in the two proposed catalytic cycles (see Figure 10).

As seen in Figure 10, the reductive elimination is the common step for the two cycles and was therefore investigated first. For the active iron catalyst, all relevant oxidation and spin states were considered. Ethyl magnesium chloride and phenyl chloride were used as model reactants. For more computational details, see Paper I. The results for the reductive eliminations that regenerate the active iron catalyst are presented in Table 3.

Table 3. Free energies in kJ/mol for the reductive elimination (RE).

"Fe"	No. of solvents[a]	Oxidation state[b]	ΔG	ΔG≠
FeMg	3	-II	195	-
FeMgCl	3	-I	94	-
Fe	2	0	30	191
FeCl	2	+I	-181	10

[a] Number of explicit dimethyl ethers used in the calculation.
[b] Oxidation state of iron after the reductive elimination.

It is evident from Table 3 that the reductive eliminations that yield iron in low oxidation states (-II or -I) are too endergonic. The Fe(III)-Fe(I) on the other hand was strongly exergonic (ΔG=-181 kJ/mol) and the Fe(II)-Fe(0) was slightly

* Computational work by Dr. J. Kleimark.

endergonic (ΔG=30 kJ/mol). However, the reaction barrier for the Fe(II)-Fe(0) reductive elimination was too high ($\Delta G^{\neq}_{RE}$=+191 kJ/mol), resulting in Fe(I) as the most plausible oxidation state ($\Delta G^{\neq}_{RE}$=+10 kJ/mol) for the active catalyst. These results, together with the experimental GC monitoring experiment, give a strong indication that complexes with Fe in lower oxidation states are not catalytically active species and that Kochi's mechanistic proposal from the early 1970's is valid.

For the Fe(III)-Fe(I) cycle, the two different cycles were considered; either the transmetalation occurs first, followed by oxidative addition and reductive elimination or oxidative addition – transmetalation – reductive elimination. It was not possible to deduce which cycle is favored from the reaction energies, or from the transition states (free energy surfaces presented in Figure 16). The oxidative addition transition states show spin polarization on the aromatic group, in good agreement with the competitive Hammett study. Oxidative addition is the rate-limiting step in both cycles, and the difference between the high points in the cycles is only 1 kJ/mol. It is possible that both pathways occur simultaneously.

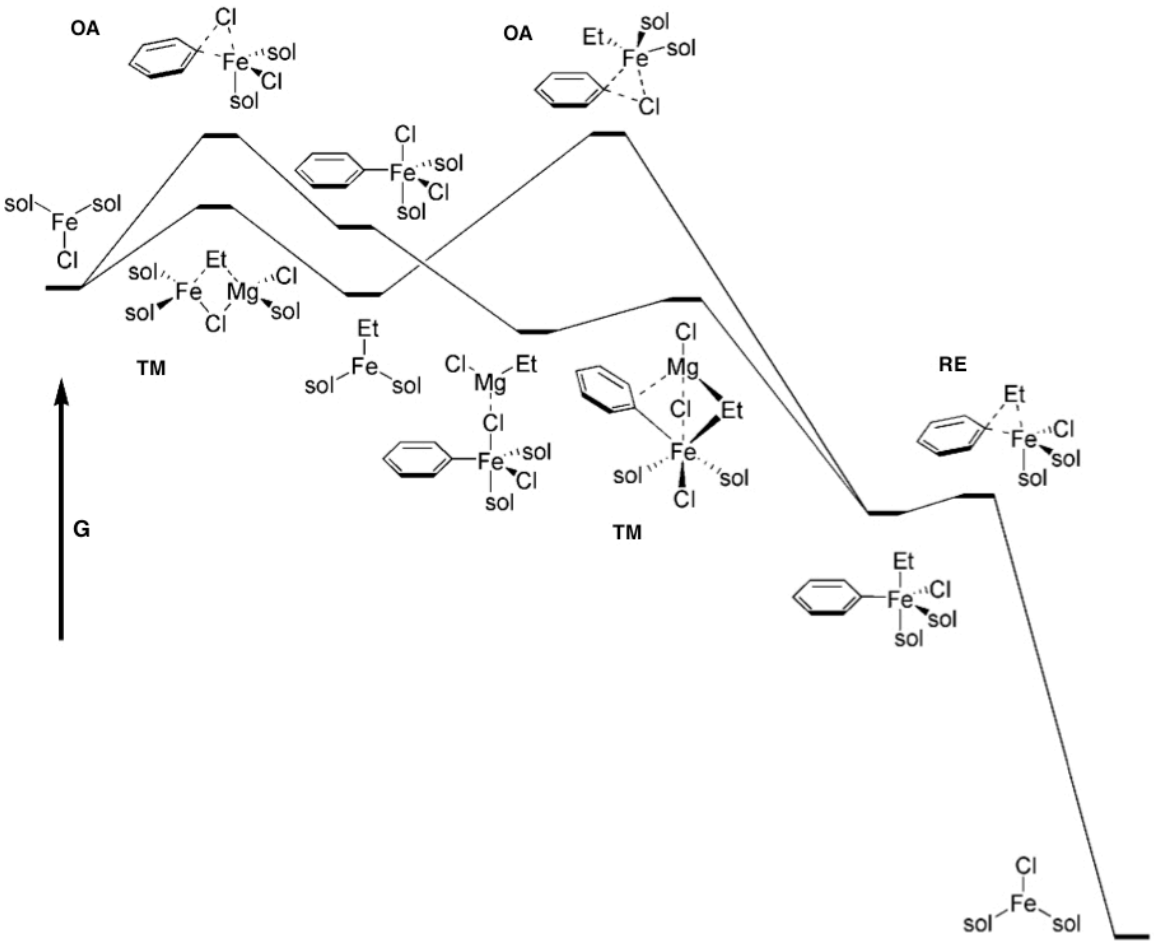

Figure 16. Free energy surface of the two catalytic cycles depicted in Figure 10. Sol=explicit solvent, OA = oxidative addition, TM = transmetalation, RE = reductive elimination.

The computational data clearly excludes the reductive elimination of Fe(II) to Fe(0) – still, the Fe(II) salts work fine in the cross coupling reaction. If Fe(II) is only a precatalyst, how does it enter the catalytic cycle? Based on the experimental results, we suspected that oligomerization was a factor. Indeed, calculations supported the reductive elimination from an Fe(II) species assisted by an Fe(II) salt to the coupled product producing two new Fe(I) species that can enter another cycle (Scheme 11).

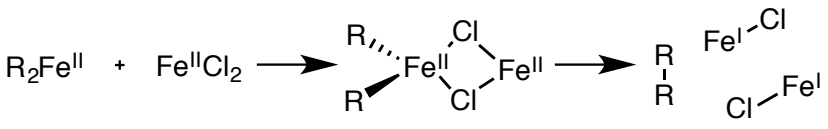

Scheme 11. Dimerization of Fe(II) species, resulting in Fe(I) species that can enter the catalytic cycle.

Iron complexes with oxidation state –II have been used in cross coupling reactions with good yields.[36, 50] However, according to our calculations, the energy barrier for the Fe(0)-Fe(-II) reductive elimination is too high. We therefore suggest that Fe(-II) is a precatalyst, that can enter the catalytic cycle after two fast oxidative additions ($[Ar_2Fe^{II}]$) and dimerization of the oxidized complexes, similar to the reaction in Scheme 11 (with an aryl group on iron instead of Cl, $[ArFe^{I}]$).

7.2. *Paper II*: Low temperature kinetic study

Iron catalyzed cross coupling reactions have a rare feature: they can run at dry ice temperature.[36, 50, 51] This ability can be very useful when improving regio- and enantioselectivity and functional group tolerance. The coupling of alkyl halide and aryl Grignard reagent was therefore studied at low temperature.

7.2.1. Reactivity at low temperature

To study the cross coupling at lower temperatures, a selection of aryl electrophiles were chosen and coupled with Grignard reagent at different temperatures: -78°C, -20°C and at room temperature (see Figure 17).* The reaction was executed according to the standard titration procedure described previously in this thesis (Scheme 9), to avoid catalyst deactivation. The reaction was monitored by GC and judged to be successful if >50 % product could be observed after the last addition.

* Experimental work performed by M. Sc. P. Emamy.

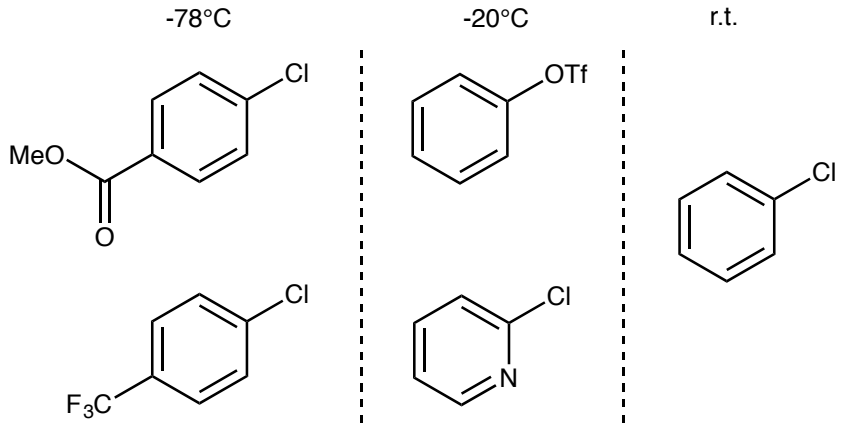

Figure 17. Competent electrophiles at different temperatures.

The aryl chlorides with strong EWG where competent substrates at -78°C. The high reactivity for these species has been observed before (see section *7.1.2.*). At -20°C, coupling of phenyl triflate and chloropyridine worked, but not phenyl chloride – the triflate is a better leaving group than chloride. The results strongly support the oxidative addition as the rate-limiting step.

7.2.2. Computational investigation of the oxidative addition

To support and explain the experimental substrate screening, DFT calculations of the oxidative addition were performed.* The barriers for the substrates to add to Fe(I) were calculated: the highest barrier was found for phenyl chloride, the one substrate that only reacted at room temperature. The barriers for the phenyl triflate and the *p*-trifluoromethyl phenyl chloride were lower, as expected from the screening. However, the barrier calculated for chloropyridine was the lowest – but no coupling product was observed at -78°C. This could be due to the coordinating ability of the nitrogen lone pair, resulting in complexation with iron or magnesium in geometries that slows down the oxidative addition.

7.2.3. Kinetics at low temperature

An initial rate study was performed on the reaction in Scheme 12.† The reaction progress was followed up to *ca.* 10 % conversion – the plots should be linear

* Computational work by Dr. J. Kleimark.
† Experimental work by Dr. P.-F. Larsson and Dr. J. Kleimark.

under these conditions, unless the mechanism changes during the course of the reaction.

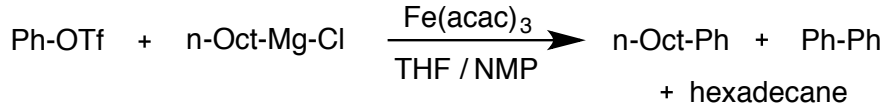

Scheme 12. Reaction utilized for the initial rate study.

Assuming that the oxidative addition is the rate-limiting step (Paper I), we would expect the reaction to be first order in substrate and catalyst, and zero or first order in the Grignard reagent, depending on if the transmetalation occurs before or after the oxidative addition.

The results were not straightforward, and somewhat surprising. For both the iron salt and the Grignard reagent, the reaction order was positive at low concentrations, indicating their involvement in the rate-limiting step. At higher concentrations, the kinetic plots had a distinct curvature indicating catalyst deactivation. For the iron, a rapid catalyst degradation was observed above 2.5 mM. At high iron concentrations, the risk of oligomerization and comproportionation to inactive forms of iron increases. When large excess of Grignard reagent is present in the reaction mixture, it could reduce iron to low-valent, less active species. The reaction order of the substrate phenyl triflate was positive, but at higher concentrations it showed opposite behavior from previous observations; in Paper I, large excess of aryl chloride prevented catalyst deactivation. Here, sudden catalyst deactivation occurred. Another catalyst deactivation path is proposed in Figure 18, where less active, diarylated Fe(II) is formed. Also, catalytically inactive poly-arylated iron complexes may form in the strongly reducing environment.[52]

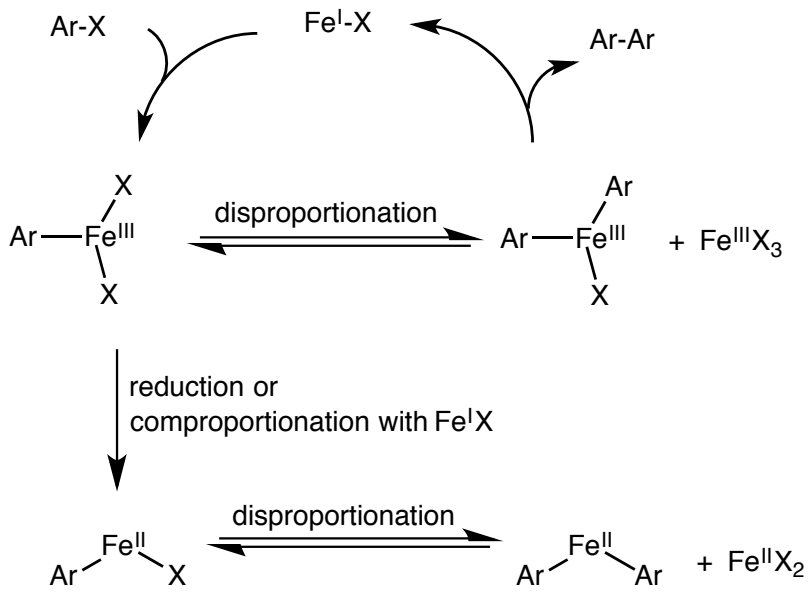

Figure 18. Formation of less active catalytically iron species.

7.2.4. Mechanism under reducing conditions

To investigate if a cycle with lower reactivity is at work (indicated by the kinetic study), the free energy surface for an Fe(0)-Fe(II) catalytic cycle was constructed using DFT. All the steps in the cycle were less efficient than in the corresponding Fe(I)-Fe(III) cycle. The energy barrier for oxidative addition was a modest 87 kJ/mol, low enough to be possible at room temperature, but the reductive elimination to yield the cross coupled product and regenerate Fe(0) was too high (204 kJ/mol). Instead, two Fe(II) species can combine and produce the more active Fe(I) complexes (see Scheme 11).

Under these reducing conditions (i.e. high Grignard concentration) we added the side path shown in Figure 19, based on the kinetic results and computational studies to the Fe(I)-Fe(III) cycle. The side path explains the catalyst deactivation at high Grignard and high catalyst concentration. It does not explain the sudden catalyst deactivation at high phenyl triflate concentrations; but this is probably due to formation of poly-arylated iron species.[52, 53]

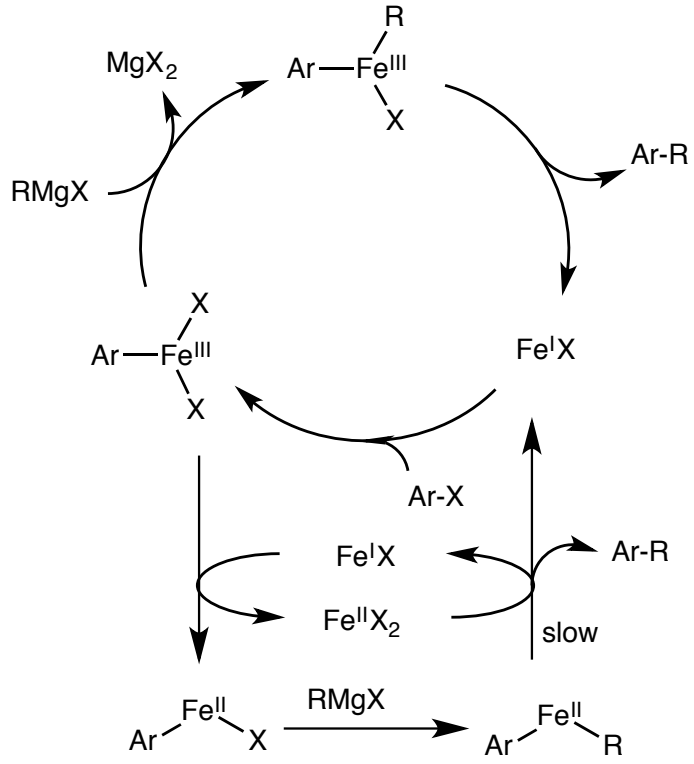

Figure 19. Fe(I)-Fe(III) catalytic cycle with hypothetical side path.

7.3. *Paper III*: Iron catalyzed coupling of aryl Grignard reagents with alkyl halides: a competitive Hammett study

The coupling of alkyl halides with aryl Grignard reagents was considered difficult, due to the low reactivity of alkyl halides in oxidative addition and the risk of β-hydride elimination.[54] However, in 2004, two groups reported iron catalyzed cross coupling of secondary alkyl halides with aryl Grignard reagents.[55] In contrast to the aryl halide – alkyl Grignard coupling, the reaction does not require any additives such as NMP or TMEDA,* probably due to the less reducing aryl Grignard reagent. The highest yield of cross coupled product and lowest amount of byproducts is obtained with diethyl ether as solvent.[55] Also, slow addition of the Grignard reagent is no longer necessary.

* Nakamura[55b,c] and Cahiez[53] have protocols with TMEDA in THF with good yields.

7.3.1. Solvent screening and "inverse addition"

The model reaction was tested in different solvent systems (see Scheme 13). Unlike the aryl halide – alkyl Grignard reaction, the phenyl Grignard is present in the reaction mixture and the substrate cyclohexyl bromide is added drop wise under 1 minute (*inverse addition*). The results are presented in Table 4. The experimental details are found in the appendix.

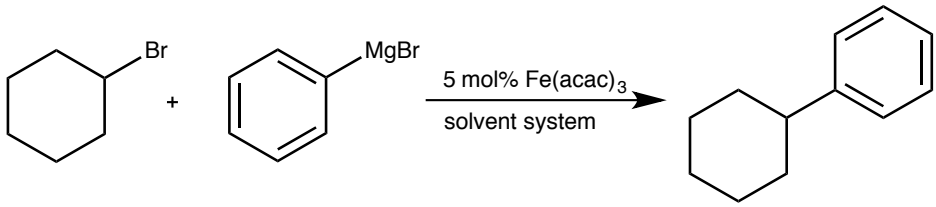

Scheme 13. Alkyl-aryl coupling in different solvents at ambient temperature.

Table 4. Different solvent systems and inverse addition vs. adding the Grignard reagent [a]

	Solvent system	Product yield [%][b]
Inverse addition	THF/NMP	26
	THF	38
	DEE/NMP	28
	DEE	83
Grignard addition	THF/NMP	53
	DEE	79

[a] Experimental work by B. Sc. Ulla Bollmann and B. Sc. Jenny Bravidor

[b] GC yields measured against internal standard (dodecane).

Diethyl ether (DEE) as the sole solvent was superior at ambient temperature. NMP inhibited the reaction in both THF and DEE. With the quick, inverse addition the reaction in DEE was finished before the sampling started (<1 minute).

7.3.2. Catalyst deactivation

In the aryl halide – alkyl Grignard coupling, catalyst deactivation was an issue – the Grignard concentration in solution was kept low and additives were needed. The deactivation could be detected visually as a darkening of the reaction mixture followed by precipitation. In the alkyl halide – aryl Grignard coupling, there is no precipitation. This feature made it possible to devise a competitive Hammett study, where the electronic effects on the aryl Grignard reagent were investigated.

7.3.3. Competitive Hammett study

With the more weakly reducing aryl Grignard reagents, the iron catalyst is active in diethyl ether without additives and at high Grignard concentrations, which enables the experimental setup displayed in Scheme 14.

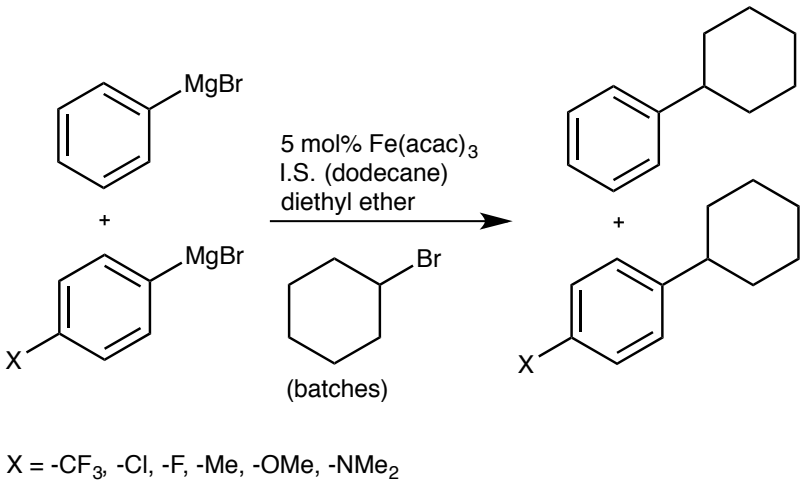

Scheme 14. Competitive Hammett study with various substituents on the aryl Grignard reagent. I.S. = internal standard.

Small portions of cyclohexyl bromide was added to a mixture of *p*-substituted and un-substituted phenyl magnesium bromide, and consumed after each addition without affecting the catalytic efficiency. Product formation was followed by GC, with samples taken before each addition of the electrophile. We assumed the same kinetic dependence for both substrates (*p*-substituted, X, and un-substituted, H) on all reagents and catalysts. With these prerequisites the relative rate, $k_{rel}=k_X/k_H$, could be obtained as the slope of the plot $\ln([X]_0/[X])$ versus $\ln([H]_0/[H])$. The initial ($[X]_0$, $[H]_0$) and the instantaneous ([X], [H]) concentrations can not be measured directly, but were calculated by comparing the instantaneous

concentration with the final product concentration after addition of the electrophile in excess. When performing a *competitive* Hammett study, only the *relative* concentrations need to be well described. Figure 20 display the plots, all with a straight line with correlation coefficient r^2 >0.99, indicating that our assumptions are correct and that possible side-reactions are negligible.

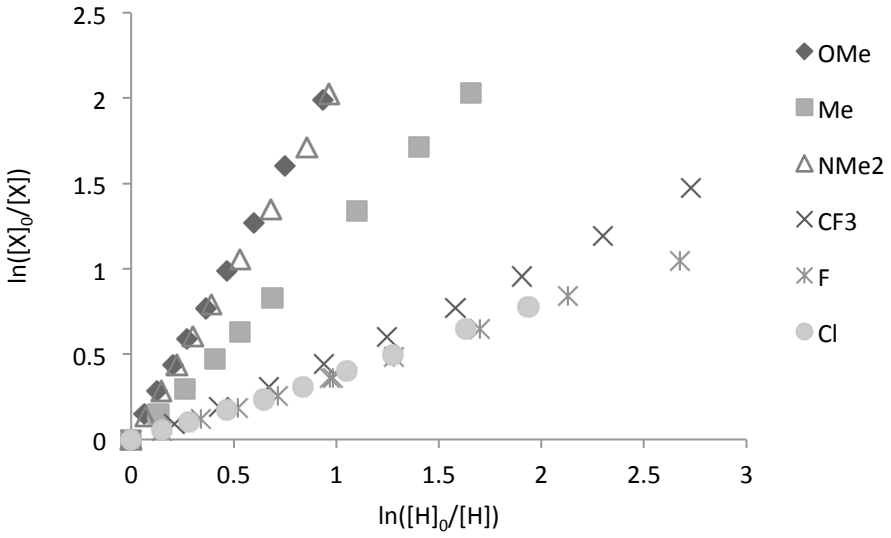

Figure 20. Plots of $\ln([X]_0/[X]) = k_{rel} \ln([X]_0/[X])$.

Even though the correlation coefficient seems good, a small curvature can be seen, for example, in the CF_3-substituted Grignard. The deviation is however too small to affect the k_{rel} value.

The relative Grignard concentrations could also be calculated from the protonation products (benzene and substituted benzene). Protonation product is generated during the acidic work-up, but is also present from the beginning in the Grignard reagents and produced in the initiation phase, and can not be used directly, but the concentrations should correlate after the initiation. By using this method, we verified that the concentration of protonation product at each point correlates well with the concentration of Grignard reagents calculated from the product formation (correlation coefficient >98 %). The relative rate for each substituted phenyl Grignard reagent was fitted to the literature σ-values by using the Hammett expression $\log(k_X/k_H)=\rho\sigma$.[13] The results are presented in Table 5 and Figure 21.

Table 5. Relative rates obtained for the *p*-substituents.

***p*-substituent**	**σ**	**k_{rel}**	**log(k_{rel})**
NMe_2	-0.83	1.99	0.3
OMe	-0.27	2.13	0.33
Me	-0.17	1.22	0.09
F	0.06	0.39	-0.41
Cl	0.23	0.39	-0.41
CF_3	0.54	0.51	-0.29

The EDG (NMe_2, OMe, Me) speeds up the reaction, while the EWG (F, Cl, CF_3) slows it down. This is in agreement with studies of transmetalation reactions in palladium catalyzed coupling reactions.[56]

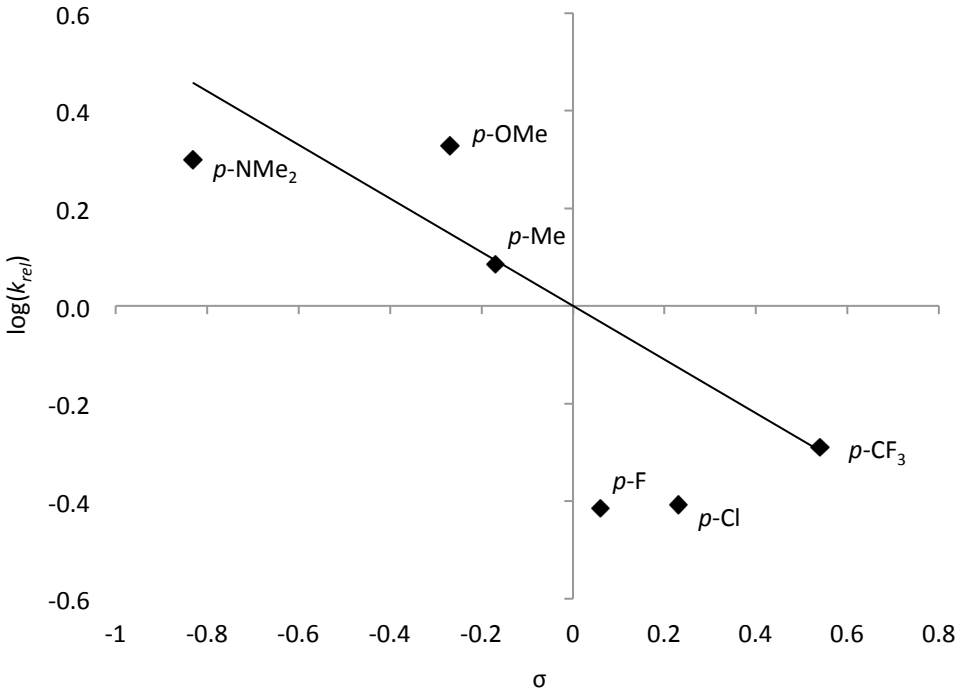

Figure 21. Hammett plot of log(k_{rel}) versus σ.

The fit in Figure 21 is not good with respect to the halide-substituted species. This is not uncommon in Hammett studies.[57] Several σ-scales, combinations of σ and Swain-Lupton parameters [58] were tested, but no statistically significant improvement was achieved.* Using the standard σ scale, $\rho \approx -0.5$, with or without

* Verified with F-test statistics.

the halides. The reductive elimination step for this reaction is the same as in the alkyl Grignard – aryl halide coupling reaction (*vide supra*). The Hammett study on the electrophile in that case gave a large positive ρ value of +3.8 – which means that the reductive elimination cannot be the rate- or selectivity determining step. Together with the computational study on the reductive elimination (section *7.1.3.*), this gives strong support for the proposed Fe(I)-Fe(III) cycle.

The NMe_2-substituent yielded a lower k_{rel} than the OMe. This type of non-linearity in Hammett plots is usually an indication that there is a switch in selectivity determining step. Most probably, the NMe_2 substituent retards one step in the catalytic cycle, increasing the barrier and making it selectivity determining. However, we cannot at this point tell which step is affected.

For the alkyl Grignard – aryl halide coupling, the TM could occur before or after the OA, with very small differences in the energy barriers for the two pathways. In this case, where we have the alkyl halide, the OA should be quite different – we could have a single electron transfer or atom transfer mechanism.[59] That would generate an alkyl radical, which could later couple either with iron or directly with the nucleophile. However, the Hammett study shows no indication of a radical being involved in the coupling step. Radical species are stabilized by all substituents, both EDG and EWG (i.e. most $\sigma^{\bullet}$ are positive) – here, we get a retardation with EWG. Radicals could still play a role in the mechanism, in the oxidative addition, providing they combine with iron before the actual coupling (see Figure 11).

In Figure 22, two different pathways are proposed, in line with the previously suggested Fe(I)-Fe(III) catalytic cycle. The two TM steps include either Fe(I) or Fe(III) and should differ in behavior with respect to the electron density on the nucleophile, something that could explain the low correlation in Figure 21 - maybe the preferred reaction path changes with the electron density.

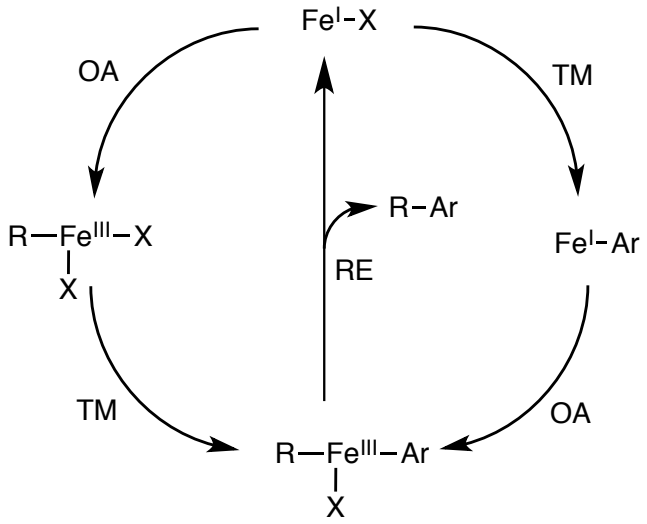

Figure 22. Mechanistic proposal with two pathways: transmetalation (TM) followed by oxidative addition (OA), or OA followed by TM. Reductive elimination (RE) yields the product and regenerates the active catalyst.

7.4. *Paper IV*: On the oxidation state of iron in iron-mediated C-C couplings[*]

To ascertain the oxidation state of iron in coupling reactions we turned to the stoichiometric homocoupling reaction originally studied by Kharasch *et al*[26, 27, 28] in the 1940's (see section 5.1.). The simple system containing only aryl Grignard and iron salt in solvent was utilized to elucidate the nature of the catalytically active iron species.

7.4.1. Stoichiometric iron reduction

The reduction of iron was investigated in a titration experiment according to Scheme 15.

[*] Experimental work by M. Sc. E. Lindstedt

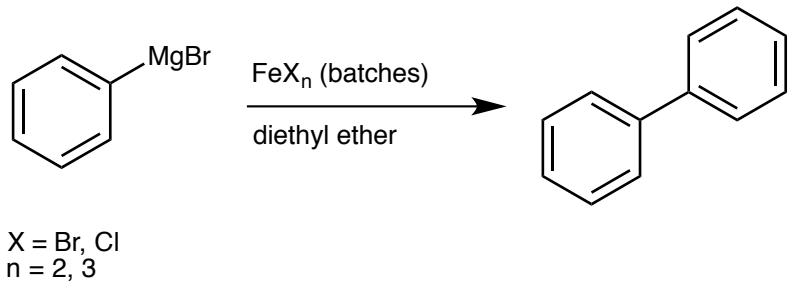

Scheme 15. Reduction of iron salt by phenyl magnesium bromide.

The iron salt was dissolved in THF and added in batches to the phenyl Grignard reagent in diethyl ether. Biphenyl formation was followed by GC, with samples taken before each addition (see Figure 23). Inert work-up of the samples proved crucial for high reproducibility (see Paper IV for description of the inert work-up). If the reduced mixture is exposed to air, the oxygen might act as oxidant and result in a higher amount of biphenyl after each iron salt addition, than possible from the stoichiometric reaction alone.[60]

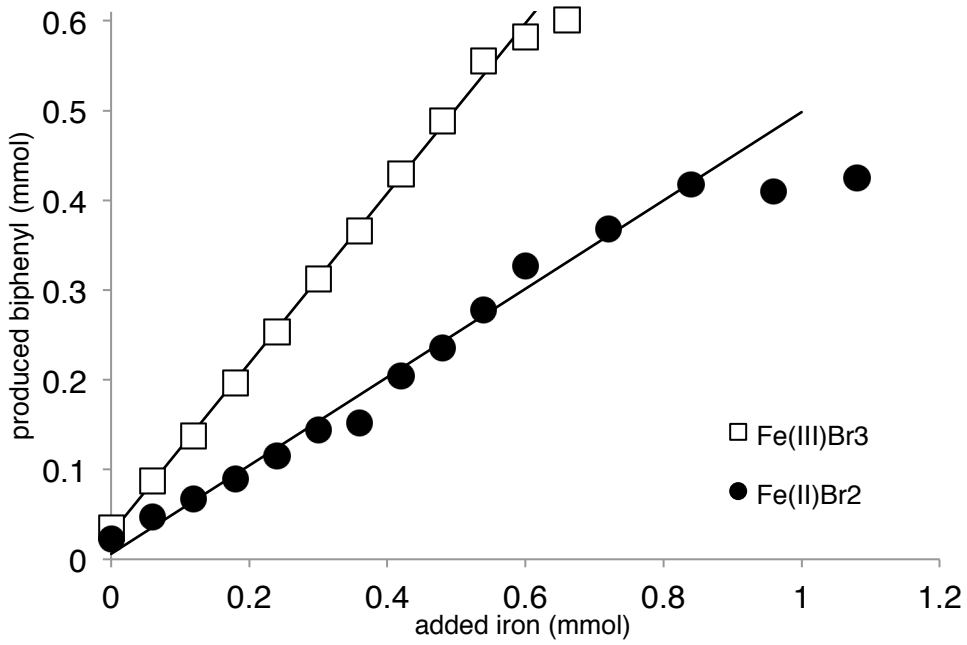

Figure 23. Biphenyl formation on titration with $FeBr_3$ and $FeBr_2$.

The biphenyl formation is followed until all Grignard reagent is consumed. The mass balance in the titration experiment was checked by also monitoring the formation of benzene. No other phenyl-containing species were detected (>95%

phenyl accounted for). The slope, corresponding to the stoichiometry of the reaction, was measured in the initial linear region, determined by F-test analysis. The titration study was performed with $FeCl_3$, $FeBr_3$ and $FeBr_2$ of at least 98 % purity. $FeCl_2$ was excluded due to solubility issues. Also, the convenient non-hygroscopic $Fe(acac)_3$ was excluded from the investigation when a number of byproducts from addition of Grignard to the acac-ligand were detected on the GC. The results are presented in Table 6.

Table 6. Slope and linearity of biphenyl formation for different iron salts

Iron salt	Purity	Slope	r^2
$FeBr_3$	98 %	0.95	0.999
$FeCl_3$	98 %	0.997	0.996
	99.99 %	1.03	0.977
$FeBr_2$	99.99 %	0.596	0.993
		0.603	1.00
		0.492	0.987

The data for the Fe(III) salts clearly show a reproducible stoichiometry close to 1. Highly pure $FeCl_3$ (99.99%) gives same result as the lower grade salt, indicating that the trace metals in commercial iron salts (e.g. copper and nickel) are not responsible for the homocoupling.[61] Formation of biphenyl from Grignard reagent is a two-electron process: the obtained data gives a strong indication that the precatalysts are reduced to Fe(I) in the presence of excess aryl Grignard and no further. Similar data was recently published by Bedford.[48]

The lower reproducibility for the Fe(II) salt is to be expected: the salt is easily oxidized to Fe(III) upon contact with air, resulting in a steeper slope. Still, the data is fairly close to 0.5, corresponding to a reduction to Fe(I). We acknowledge that the diaryl-Fe(II) complex cannot yield Fe(I) with a normal reductive elimination – that requires two electrons. However, we have previously shown that a diorgano-Fe(II) in a bimetallic complex can undergo a reductive

elimination (with slightly higher barrier), resulting in two Fe(I) species (see section *7.1.3.*, or Paper I).

7.4.2. Active catalyst

To prove that the reduced iron in the presence of excess Grignard is catalytically active, the experiment in Scheme 16 was conducted.

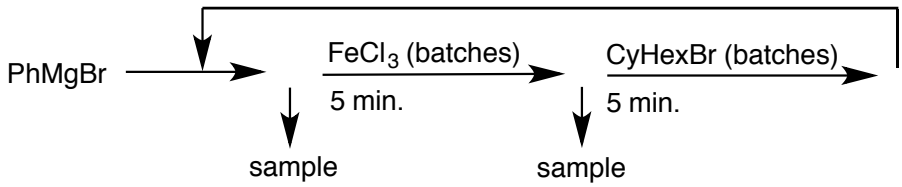

Scheme 16. Alternating catalyst generation and cross coupling.

The alkyl electrophile cyclohexyl bromide was added to the reaction mixture in between the iron salt additions. Cross coupled product (phenyl cyclohexane) was observed upon every addition of the alkyl bromide – and after each iron salt addition, homocoupled product was observed. The data from this titration experiment is presented in Figure 24.

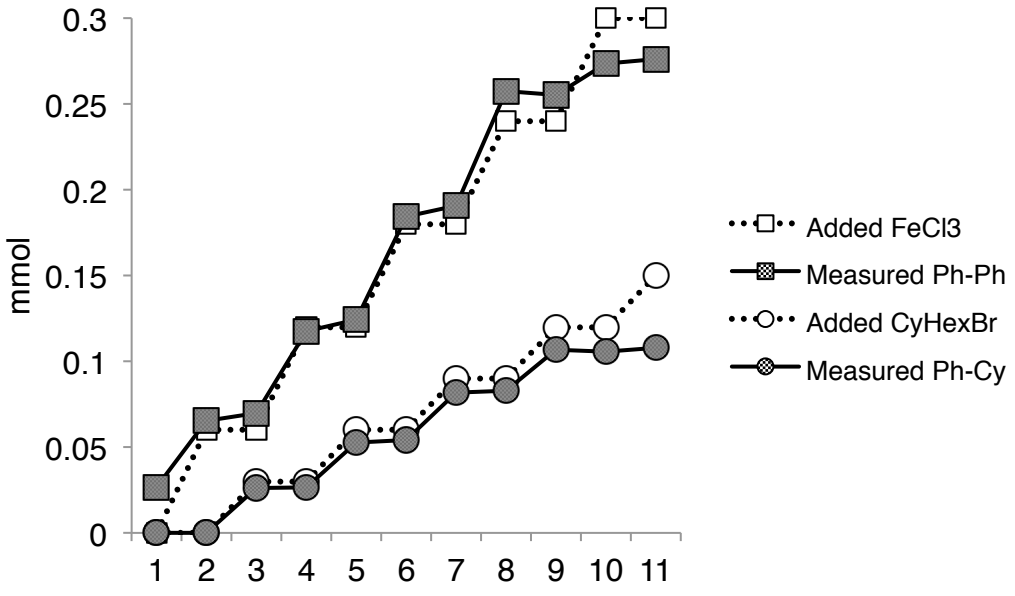

Figure 24. Monitoring of product generated from alternating addition of $FeCl_3$ and cyclohexyl bromide.

Addition of iron salt gives only biphenyl, and addition of cyclohexyl bromide only yields the phenyl cyclohexane. The addition before sample 10 consumes all the phenyl magnesium bromide, and no further increase in products can be seen. Also, unreacted cyclohexyl bromide is now detected in the reaction mixture.

7.4.3. Proposed reaction mechanisms

Starting from Fe(III), the following reaction mechanism is suggested for the homocoupling: two consecutive transmetalations (TM) gives a diarylated Fe(III) complex. The diaryl-Fe(III) can either undergo a third TM to a poly-arylated species followed by a reductive elimination (RE) to yield biphenyl and aryl-Fe(I) (path i) or a RE to yield biphenyl and Fe(I)-bromide (path ii). The Fe(I)-bromide can than undergo TM to aryl-Fe(I). The complexes in Scheme 17 are stabilized by solvent molecules (omitted for clarity). We were unable to differentiate between the two paths based on the kinetic studies, so the proposed mechanisms were further investigated by DFT calculations.

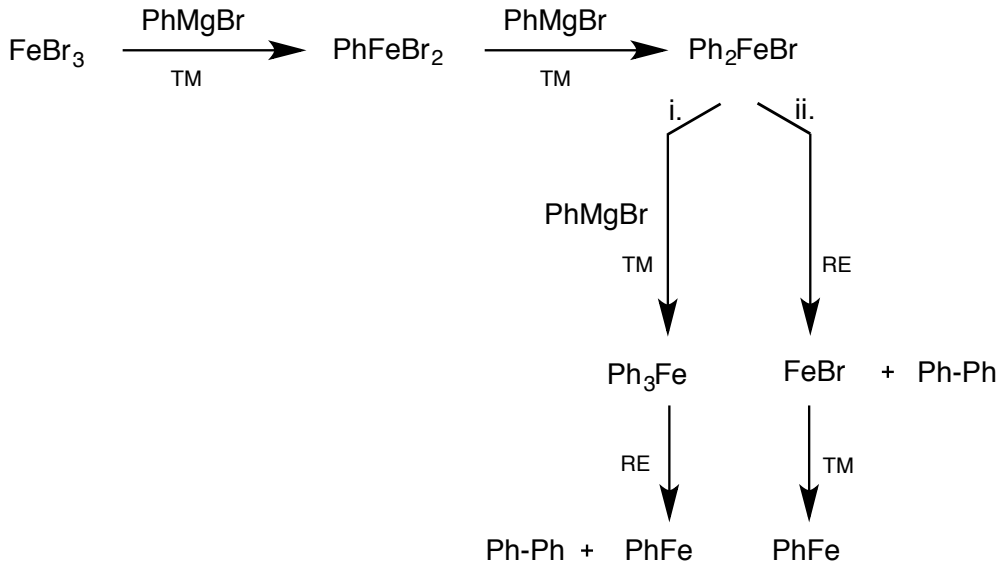

Scheme 17. Suggested reaction mechanisms for the homocoupling of aryl Grignard reagent.

7.4.4. Computational study

To investigate the postulated mechanism, dispersion-corrected DFT methods were used (B3LYP-D3/LACVP*). All energies are free energies in solvent (for details, see Paper IV). The free energy surfaces are presented in Figure 26. For each iron complex all plausible spin states were calculated. The number of explicit solvent molecules (dimethyl ether as model solvent) was determined by the free energy. For the TM steps, we assumed that the association of Grignard reagent to the iron complexes and the dissociation of the magnesium halide from the complex, would have low barriers (see Paper I) and we only calculated the bimetallic iron/magnesium complexes with a bridging phenyl group (Fe-μ-Ph-Mg). The bimetallic complexes with the lowest free energies required the dissociation of one solvent molecule from each metal: the dissociation costs enthalpy, but the cost is compensated by a gain in entropy. The first TM occurs at a high spin Fe(III), but the transfer of the aryl group with a strong ligand field is enough to induce a spin change to the favored intermediate spin (from S=5/2 to S=3/2).[62] All arylated Fe complexes in this study were found to prefer S=3/2. An intermediate spin is rarely seen.[63] The unsymmetrical field around iron with only one strong field ligand results in the increase in energy of one d-orbital, making it possible to attain the intermediate spin (see Figure 25).

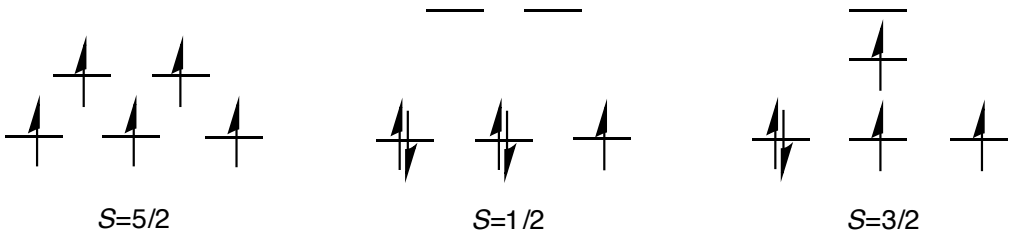

Figure 25. Spin states for a d^5 complex. The first two are based on octahedral geometry: a weak field gives a high spin complex, a strong field gives low spin. If there is only one strong field ligand present, an intermediate spin may appear.

After the second TM, the diarylated Fe(III) complex can either undergo a third TM (path i) or RE (path ii). A third TM is an endergonic step, while the RE is strongly exergonic. The phenyl groups in the diarylated Fe(III) complex are in perfect position for the RE. The potential energy barrier is only 1 kJ/mol, and the

transition state is lower than the reactant on the free energy surface. This is a computational artifact almost always apparent when potential energy barriers are low.

A bimolecular reaction will always have a free energy barrier - if the barrier cannot be found on the potential energy surface, the reaction is diffusion-controlled and will have a free energy barrier of at least 20 kJ/mol.[64]

Clearly, the mechanism follows path ii, where all steps are exergonic and the potential energy barriers are low. After the RE, the high spin Fe(I) bromide (S=3/2) can be transmetalated to aryl-Fe(I).

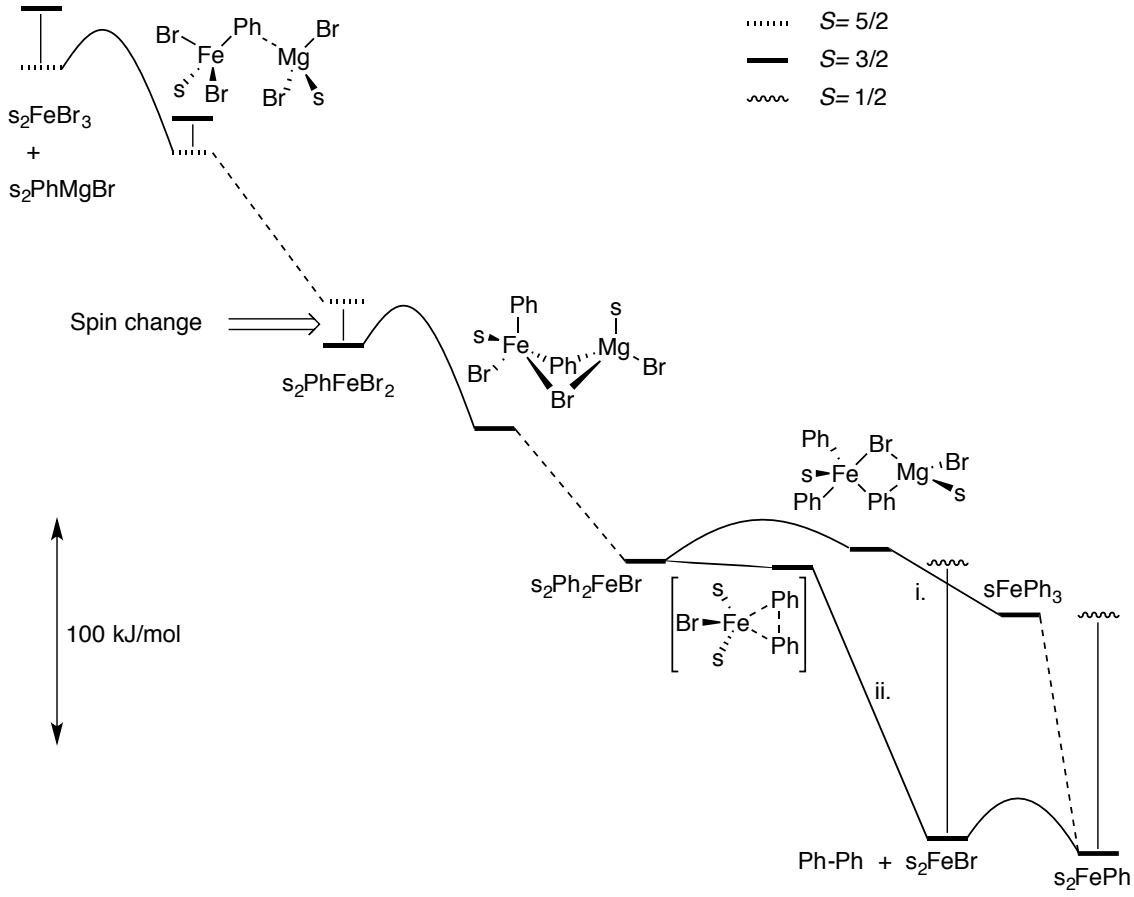

Figure 26. Free energy surfaces for the homocoupling reaction of PhMgBr mediated by $FeBr_3$. The curves represent energy barriers of at least 20 kJ/mol, the dashed lines are dissociations and "s" is explicitly added dimethyl ether.

8. Conclusions

The combination of experimental and theoretical methods proved to be a powerful tool in elucidating reaction mechanisms. The results of the mechanistic investigations of the iron catalyzed C-C coupling reaction have been presented and discussed in this thesis. Iron is a very versatile transition metal, with an extraordinary ability to be an active catalyst at dry ice temperature and to couple all kinds of combinations of sp^2 and sp^3 nucleophiles and electrophiles.

The most plausible reaction mechanism for the iron catalyzed cross coupling of alkyl Grignard and aryl halide is an Fe(I)-Fe(III) cycle, consisting of oxidative addition, transmetalation and reductive elimination. The Fe(I) complex undergoes a rate-limiting oxidative addition to the aryl halide, and a rapid transmetalation either before or after the oxidative addition yields an Fe(III) complex, with the alkyl and aryl-groups attached. The subsequent reductive elimination gives the cross coupled product and regenerates the active Fe(I) catalyst. The Fe(I) catalyst can be stabilized by dilution or by adding chelating ligands (such as NMP or TMEDA). An excess of alkyl Grignard reagent may overreduce iron to more inactive complexes. Slow addition of the Grignard reagent can prevent this catalyst deactivation.

The coupling of aryl Grignard and alkyl halide follows the same mechanism as above. The aryl Grignard is less reducing than the alkyl counterpart, allowing rapid addition of Grignard to the reaction mixture, or even inverse addition, without the risk of catalyst deactivation. Coordinating ligands or co-solvents like NMP inhibits the reaction. A simple reaction protocol with the alkyl halide, aryl Grignard and iron salt in diethyl ether works best. The aryl Grignard reagent can only reduce iron salts to Fe(I) and no further, avoiding the risk of overreduction.

The combination of experimental and computational evidence has been very powerful in elucidating the details of the different mechanistic possibilities studied in this thesis. A key factor has been the choice of compatible experimental and computational methods. Isolation of single reaction steps, such as in the aryl

homocoupling, or competitive kinetic studies such as Hammett, allows a very precise application of computational comparisons between closely related species. The resulting error cancellation is very important for obtaining high accuracy in computational predictions.

Iron catalyzed cross coupling reactions are in many cases good alternatives to the palladium and nickel catalyzed counterparts. Iron salts are generally cheap, environmentally benign and have low toxicity. New methodologies are being developed, based on the increasing mechanistic knowledge. The results presented here can assist in the development of improved reaction protocols.

9. Acknowledgements

En doktorandtjänst omfattar ganska många år, och det finns många personer som jag vill tacka för att ni stöttat mig, berört mig, lyst upp min dag och bidragit till att den här avhandlingen har blivit skriven – tack!

Till min handledare **Per-Ola Norrby**; PeO, sluta aldrig upp med att engagera och entusiasmera! Vem vet, hade inte du dykt upp på våningen hade jag nog hållit på med något annat nu… ☺

Min examinator **Göran Hilmersson**, för givande samtal under åren.

Tack till **Göteborgs Universitet** för att ni tog emot mig som doktorand. Tack till **Vetenskapsrådet** och **AstraZeneca** för projektfinansiering. Tack **ÅForsk**, **Kungliga Vetenskaps- och Vitterhets-samhället**, **Adlerbertska**, **Helge Ax:son Johnsons Stiftelse**, **Kemistsamfundet** och **COST D40** för era generösa resebidrag till konferenser och sommarskolor.

Tidigare och nuvarande gruppmedlemmar: **Jonatan** och **Per-Fredrik**, tack för gott samarbete, rumssällskap, resesällskap, lån av icke-kemi relaterade böcker (Jonatan), tips och diskussioner om film och serier (Per-Fredrik). Doktorandtiden hade inte blivit densamma utan er! **Carina**, **Charlotte**, **Sten**, **Petra** och **Elaine**: tack för trevligt sällskap och givande diskussioner. **Erik**, vilken arbetsmyra du är – tack för ditt hårda jobb inne på labbet. Tack till studenterna som jobbat i labbet under åren: **Kenan**, **Parisa**, **Jenny**, **Ulla** och **Irma**. Tack **CJ** för trevligt rumssällskap.

Örjan Hansson, tack för gott samarbete och givande diskussioner.

Anders Lennartson för gott samarbete genom åren (några pek blev det!), avhandlingstips, korrekturläsning och trevligt sällskap.

Johan Eriksson, tack för all hjälp genom åren med i princip allt möjligt. Våningen är inte densamma utan sin hustomte ☺.

Tack **alla på våning 8 och 9** för fikapauser, kräftskivor, julmiddagar, oktoberfest, och annat kul genom åren.

Sabumnim **Georg**, jag hade inte varit den jag är idag utan din vägledning. Tack för hård fysisk och mental träning.

Mina goa vänner, som kanske inte riktigt förstår vad jag gör, men alltid ställer upp för mig och bjuder på många skratt, vin, spelkvällar, lilla julafton, midsomrar, överraskningsfester och annat underbart ☺.

Min familj, tack för att ni stöttat mig och alltid ställer upp för mig, vad det än gäller. Jag tror en stor del av avhandlingen blev skriven i Emmys lägenhet, eller under helger då Astrid var i Ytterby!

Mikael och **Astrid**; finns inga ord som beskriver min kärlek och tacksamhet till er.

Appendix

Experimental procedures (for section 7.3.1)

A) "Inverse" addition

A dry round bottomed flask was sealed with a rubber septum, then evacuated and refilled with nitrogen four times. The flask was charged with dry solvent (7 mL), distilled dodecane (225 μL, 1 mmol) and phenyl magnesium halide (0.8 mL, 2.4 mmol, 3 M). A mixture of cyclohexyl bromide (123 μL 1 mmol), $Fe(acac)_3$ (mg, 0.05 mmol) dry solvent (3 mL) and co-solvent (0.33 mL distilled NMP) was added via a syringe to the flask during <1 minute. Directly after addition, an aliquot (0.2 mL) was taken from the mixture, quenched with saturated NH_4Cl (0.5 mL), filtered through a small silica plug, diluted with DEE and analyzed by GC (dodecane was used as the internal standard). Every 3 minutes a sample was taken, until a total of 10 samples were collected.

B) Grignard addition

A dry round bottomed flask was sealed with a rubber septum, then evacuated and refilled with nitrogen four times. The flask was charged with cyclohexyl bromide (0.62 mL 5 mmol), dry solvent (50 mL), distilled dodecane (1.12 mL, 5 mmol) and co-solvent (distilled NMP, 1.15 mL). The phenyl magnesium halide (0.4 mL, 12 mmol, 3 M) was added to the reaction mixture in portions of 0.6 mmol. 5 minutes after each portion, a small sample (0.2 mL) was withdrawn, quenched with saturated NH_4Cl (0.5 mL), filtered through a small silica plug, diluted with DEE and analyzed by GC (dodecane was used as the internal standard).

References

1. K. C. Nicolaou, P. G. Bulger, D. Sarlah, *Angew. Chem. Int. Ed.*, **2005**, *44*, 4442–4489.

2. C. W. Scheele, Kongl. Vetenskaps Academiens Nya Handl. **1782**, 3, 35-46.

3. H. M. Leicester, H. S. Klickstein: A Source Book in Chemistry 1400-1900, Harvard University Press, **1969**, pp. 265-268 (Berzelius) pp. 491-493 (Ostwald).

4. a) J. Hartwig, Organotransition Metal Chemistry, University Science Books, Sausalito, **2010** b) D. J. Berrisford, C. Bolm, K. B. Sharpless, Angew. Chem. Int. Ed. Engl., **1995,** 34, 1059–1070.

5. For an overview of the use of transition metals in organic reactions: M. Beller, C. Bolm, Transition Metals for Organic Synthesis, vol. 2, Wiley-VCH, Weinheim, **2004.**

6. IUPAC. Compendium of Chemical Terminology, 2nd ed. (the "Gold Book"). Compiled by A. D. McNaught and A. Wilkinson. Blackwell Scientific Publications, Oxford, **1997**.

7. D. Forster, *Adv. Organomet. Chem.* **1979**, *17*, 255−267.

8. K. Tamao, K. Sumitani, M. Kumada, *J. Am. Chem. Soc.* **1972**, 94, 4374-4376.

9. R. J. P. Corriu, J. P. Masse, *J. Chem. Soc. Chem. Commun*. **1972**, 144a.

10. http://www.nobelprize.org/nobel_prizes/chemistry/laureates/2010/

11. R. B. Jordan, *Reaction Mechanisms of Inorganic and Organometallic Systems*, 3rd ed. Oxford University Press, Inc. **2007**.

12. L. P. Hammett, *J. Am. Chem. Soc.* **1937**, *59*, 96-103.

13. a) C. Hansch, A. Leo, R. W. Taft, *Chem. Rev.* **1991**, *91*, 165-195; b) X. Creary, M. E. Mehrsheikhmohammadi, S. Mcdonald, *J. Org. Chem*. **1987**, *52*, 3254-3263.

14. a) H. Man Yau, A. K. Croft, J. B. Harper, *Chem. Commun.* **2012**, *48*, 8937-8939; b) P. Fristrup, L. Bahn Johansen, C. H. Christensen, *Chem. Commun.* **2008**, 2750-2752.

15. C. J. Cramer, *Essentials of Computational Chemistry: Theories and Models*, 2nd ed. Wiley-VCH, Weinheim, **2004**.

16. a) A. D. Becke, *J. Chem. Phys.* **1993**, *98*, 5648-5652; b) A. D. Becke, *J. Chem. Phys.* **1993**, *98*, 1372-1377.

17. a) C. T. Lee, W. T. Yang, R. G. Parr, *Phys. Rev. B.* **1988**, *37*, 785-789; b) P. J. Stephens, F. J. Devlin, C. F. Chabalowski, M. J. Frisch, *J. Phys. Chem.* **1994**, *98*, 11623-11627.

18. J. Tomasi, B. Mennucci, R. Cammi, *Chem. Rev.* **2005**, *105*, 2999-3093.

19. a) D. J. Tannor, B. Marten, R. Murphy, R. A. Friesner, D. Sitkoff, A. Nicholls, M. Ringnalda, W. A. Goddard, B. Honig, *J. Am. Chem. Soc.* **1994**, *116*, 11875-11882; b) B. Marten, K. Kim, C. Cortis, R. A. Friesner, R. B. Murphy, M. N. Ringnalda, D. Sitkoff, B. Honig, *J. Phys. Chem.* **1996**, *100*, 11775-11788.

20. S. Grimme, J. Antony, S. Ehrlich, H. Krieg, *J. Chem. Phys.* **2010**, *132*, 154104.

21. B. Plietker, *Iron Catalysis in Organic Chemistry*, Wiley-VCH, Weinheim, **2008**.

22. P. J. van Konigsbruggen, *Top. Curr. Chem.,* **2004**, *233*, p.123.

23. S. P. de Visser, D. Kumar, *Iron-Containing Enzymes: Versatile Catalysts of Hydroxylation Reactions in Nature*, Royal Society of Chemistry, Cambridge, **2011**.

24. M. D. Fryzuk, *Nature*, **2004**, *427*, 498-499.

25. C. Bolm, J. Legros, J. Le Paih, L. Zani, *Chem. Rev.* **2004,** *104*, 6217−6254.

26. M. S. Kharasch, E. K. Fields, *J. Am. Chem. Soc.* **1941**, *63*, 2316-2320.

27. a) H, Gilman, M. Lichtenwalter, *J. Am. Chem. Soc.* **1939**, *61*, 957-959; b) G. M. Bennett, E. E. Turner, *J . Chem.* Soc., **1914**, *105*, 1057-1062. For a detailed review of early results, see F. A. Cotton, *Chem. Rev.* **1955**, *55*, 551-594.

28. M. S. Kharasch; O. Reinmuth, *Grignard reaction of Nonmetallic Substances*, Prentice-Hall, New York, **1954**.

29. M. H. Abraham, M. J. Hogarth, *J. Organomet. Chem.* **1968**, *12*, 497-515.

30. M. Tsutsui, *Annals of the New York Academy of Sciences*. **1961**, *93*, 133-146.

31. V. D. Parker, C. R. Noller, *J. Am. Chem. Soc.* **1964**, *86*, 1112-1116.

32. M. Tamura, J. K. Kochi, *J. Organomet. Chem.* **1971**, *31*, 289-309.

33. a) M. Tamura, J. K. Kochi, *J. Am. Chem. Soc.* **1971**, *93*, 1487-1489; b) M. Tamura, J. K. Kochi, *Synthesis*, **1971**, 303; c) M. Tamura, J. K. Kochi, *Bull. Chem. Soc. Jpn.* **1971**, *44*, 3063-3073; d) M. N. Neumann, J. K. Kochi, *J. Org. Chem.* **1975,** *40*, 599-606; e) R. S. Smith, J. K. Kochi, *J. Org. Chem.* **1976**, *41*, 502-509.

34. a) G. A. Molander, B. J. Rahn, D. C. Shubert, S. E. Bonde, *Tetrahedron Lett.* **1983**, *24*, 5449-5452; b) V. Fiandanese, G. Marchese, V. Martina, L. Ronzini, *Tetrahedron Lett.* **1984**, *25*, 4805-4808; c) D. J. Evans, R. A. Henderson, A. Hills, D. L. Hughes, K. E. Oglieve, *J. Chem. Soc., Dalton Trans.* **1992**, 1259-1265; d) T. Kauffmann, K. U. Voss, G. Neiteler, *Chem. Ber.* **1993,** *126,* 1453-1459.

35. G. Cahiez, H. Avedissian, *Synthesis* **1998**, 1199-1205.

36. A. Fürstner, A. Leitner, M. Mendez, H. Krause, *J. Am. Chem. Soc.* **2002**, *124*, 13856-13863.

37. A. E. Jensen, W. Dohle, I. Sapountzis, D. M. Lindsay, V. A. Vu, P. Knochel, *Synthesis* **2002**, 565-569.

38. For a review: a) W. M. Czaplik, M. Mayer, J. Cvengroš, A. J. von Wangelin, *ChemSusChem*, **2009**, *2*, 396–417. For Fe-catalyzed aryl-aryl cross coupling: b) T. Hatakeyama, M. Nakamura, *J. Am. Chem. Soc*, **2007**, *129*, 9844-9845; c)I. Sapountzis, W. Lin, C. Kofink, C. Despotoulou, P. Knochel, *Angew. Chem. Int. Ed.* **2005**, *44*, 1654-1658; d) C. Kofink, B. Blank, S. Pagano, N. Götz, P. Knochel, *ChemComm.* **2007**, 1954-1956. e)

S. Gülak, A. Jacobi von Wangelin, Angew. *Chem. Int. Ed.*, **2012**, *51*, 1357–1361. For Fe-catalyzed alkyl-alkyl coupling: f) K. G. Dongol, H. Koh, M. Sau, C. L. L. Chai, *Adv. Synth. Catal.* **2007**, *349*, 1015–1018; g) M. Guisan-Ceinos, F. Tato, E. Bunuel, P. Calle, D. J. Cardenas, *Chem. Sci.*, **2013**, 4, 1098–1104.

39. a) B. D. Sherry, A. Fürstner, *Acc. Chem. Res.*, **2008**, *41*, 1500–1511; b) A. Leitner, *Iron-Catalyzed Cross-Coupling Reactions, in Iron Catalysis in Organic Chemistry: Reactions and Applications* (ed B. Plietker), Wiley-VCH, Weinheim **2008**; c) W. M, Czaplik, M. Mayer, S. Grupe, A. J. von Wangelin, *Pure Appl. Chem.* **2010**, *82*, 1545-1553

40. a) M. Nakamura, K. Matsuo, S. Ito, E. Nakamura, *J. Am. Chem. Soc.* **2004**, *126*, 3686-3687; b) R. B. Bedford, D. W. Bruce, R. M. Frost, M. Hird, *Chem. Commun.* **2005**, 4161-4163; c) A. Guerinot, S. Reymond, J. Cossy, *Angew. Chem., Int. Ed.* **2007**, *46*, 6521-6524; d) R. B. Bedford, M. Betham, D. W. Bruce, A. A. Danopoulos, R. M. Frost, M. Hird, *J. Org. Chem.* **2006**, *71*, 1104-1110.

41. Q. Ren, S. Guan, F. Jiang, J. Fang, *J. Phys. Chem. A*, **2013**, *117*, 756-764

42. a) A. Fürstner, A. Leitner, *Angew. Chem., Int. Ed.* **2002**, *41*, 609-612; b) R. Martin, A. Fürstner *Angew. Chem., Int. Ed.* **2004**, *43*, 3955−3957; c) A. Fürstner, R. Martin, H. Krause, G. Seidel, R. Goddard, C. W. Lehmann, *J. Am. Chem. Soc.* **2008,** *130*, 8773-8787.

43. K. Jonas, L. Schieferstein, C. Krüger, Y.-H. Tsay, *Angew. Chem. Int. Ed. Engl.*, **1979**, *18*, 550–551.

44. a) L. E. Aleandri, B. Bogdanovic, P. Bons, C. Duerr, A. Gaidies, T. Hartwig, S. C. Huckett, M. Lagarden, U. Wilczok, R. A. Brand, *Chem. Mater.* **1995**, *7*, 1153-1170; b) L. E. Aleandri, B. Bogdanovic, P. Bons, C. Duerr, D. J. Jones, J. Roziere, U. Wilczok, *Adv. Mater.* **1996**, *8*, 600-604. c) B. Bogdanovic, M. Schwickardi, *Angew. Chem. Int. Ed.*, **2000**, *39*, 4610–4612.

45. C.L. Kwan, J. K. Kochi, *J. Am. Chem. Soc.* **1976**, *98*, 4903-4912.

46. M. Gargano, P. Giannoccaro, M. Rossi, G. Vasapollo, A. Sacco, *J. Chem. Soc. Dalton. Trans. 1975*, 9-12.

47. E. L. Muetterties, B. A. Sosinski, K. I. Zamaraev, *J. Am. Chem. Soc.* **1975**, *97*, 5299-5300.

48. C. J. Adams, R. B. Bedford, E. Carter, N. J. Gower, M. F. Haddow, J. N. Harvey, M. Huwe, M. Á. Cartes, S. M. Mansell, C. Mendoza, D. M. Murphy, E. C. Neeve, J. Nunn, *J. Am. Chem. Soc.* **2012**, *134*, 10333-10336.

49. For coupling of non-activated aryl chlorides, see: M. C. Perry, A. N. Gillett, T. C. Law, *Tetrahedron Letters* **2012**, *53*, 4436–4439.

50. a) R. Martin, A. Fürstner *Angew. Chem., Int. Ed.* **2004**, *43*, 3955−3957; b) A. Fürstner, R. Martin, H. Krause, G. Seidel, R. Goddard, C. W. Lehmann, *J. Am. Chem. Soc.* **2008,** *130*, 8773-8787.

51. a) J. Quintin, X. Franck, R. Hocquemiller, B. Figadere, *Tetrahedron Lett.* **2002**, 43, 3547–3549; b) R. Martin, S. L. Buchwald, *J. Am. Chem. Soc.* **2007**, *129*, 3844–3845; c) O. Vechorkin, X. L. Hu, *Angew. Chem. Int. Ed.* **2009**, *48,* 2937-2940; e) S. Lou, G. C. Fu, *J. Am. Chem. Soc.* **2010**, *132*, 1264– 1266; f) J. Adrio, J. C. Carretero, *ChemCatChem*, **2010**, *2*, 1384-1386.

52. P. J. Alonso, A. B. Arauzo, J. Fornies, M. A. Garcia-Monforte, A. Martin, J. I. Martinez, B. Menjon, C. Rillo, J. J. Saiz-Garitaonandia, *Angew. Chem., Int. Ed.* **2006**, *45*, 6707-6711.

53. G. Cahiez, V. Habiak, C. Duplais, A. Moyeux, *Angew. Chem. Int. Ed.* **2007**, *46*, 4364-4366

54. A. C. Frisch, M. Beller, *Angew. Chem. Int. Ed.* **2005**, *44*, 674-688.

55. a) T. Nagano, T. Hayashi, *Org. Lett.* **2004**, *6*, 1297-1299; b) M. Nakamura, K. Matsuo, S. Ito, E. Nakamura, *J. Am. Chem. Soc.* **2004**, *126*, 3686-3687; c) T. Hatakeyama, S. Hashimoto, K. Ishizuka, M. Nakamura, *J. Am. Chem. Soc.* **2009**, *131*, 11949-11963.

56. a) V. Farina, B. Krishnan, D. R. Marshall, G. P. Roth, *J. Org. Chem.* **1993**, *58*, 5434-5444; b) T. Nishikata, Y. Yamamoto, N. Miyaura, *Organometallics* **2004**, *23*, 4317-4324; c) D. Zim, S. M. Nobre, A. L. Monteiro, *J. Mol. Catal. A* **2008**, *287*, 16-23; d) Z. B. Dong, G. Manolikakes, L. Shi, P. Knochel, H. Mayr, *Chem. Eur. J.* **2010**, *16*, 248-253.

57. D. A. Culkin, J. F. Hartwig, *Organometallics* **2004**, *23*, 3398-3416.

58. a) C. G. Swain, E. C. Lupton, *J. Am. Chem. Soc.* **1968**, *90*, 4328-4337; b) C. G. Swain, S. H. Unger, N. R. Rosenquist, M. S. Swain, *J. Am. Chem. Soc. 1983*, **105**, 492-502.

59. G. O. Jones, P. Liu, K. N. Houk, S. L. Buchwald, *J. Am. Chem. Soc.* **2010**, *132*, 6205-6213.

60. W. Liu, A. Lei, *Tetrahedron Lett.*, **2008**, *49*, 610-613.

61. P.-F. Larsson, A. Correa, M. Carril, P.-O. Norrby, C. Bolm, *Angew. Chem. Int. Ed.* **2009**, *48*, 5691-5693. See also: S. L. Buchwald, C. Bolm, *Angew. Chem. Int. Ed.* **2009**, *48*, 5586-5587; I. Thomé, A. Nijs, C. Bolm, *Chem. Soc. Rev.* **2012**, *41*, 979- 987.

62. P. J. van Konigsbruggen, Y. Maeda, H. Oshio, *Top. Curr. Chem.* **2004**, *233*, 259-324.

63. S. Mossin, B. L. Tran, D. Adhikari, M. Pink, F. W. Heinemann, J. Sutter, R. K. Szilagyi, K. Meyer, D. J. Mindiola, *J. Am. Chem. Soc.* **2012**, *134*, 13651-13661.

64. C. L. McMullin, J. Jover, J. N. Harvey, N. Fey, *Dalton Trans.* **2010**, *39*, 10833-10836.